Numerical Weather Prediction

The Tropical Behaviour of the Convective Parametrization in Aquaplanet Simulations and the Sensitivity to Timestep

Forecasting Research Technical Report No. 482

M.R. Willett and S.F. Milton

email:nwp˙publications@metoffice.gov.uk

Contents

1 Introduction **2**

2 Model systematic errors and relation to convection **3**

3 Description of the 4A convection scheme **3**
3.1 Triggering and diagnosis of convection type . . . 5
3.2 Updraughts . . . 6
3.2.1 Mass flux profile . . . 6
3.2.2 Entrainment and detrainment rates . . . 7
3.2.3 Termination . . . 8
3.2.4 Closure . . . 8
3.2.5 Precipitation . . . 9
3.3 Downdraughts . . . 9
3.3.1 Diagnosis . . . 9
3.3.2 Mass flux profile . . . 9
3.3.3 Entrainment and detrainment rates . . . 9
3.3.4 Termination . . . 9
3.3.5 Closure . . . 10
3.4 Effects of convection on the environment . . . 10

4 Aquaplanet configuration and model setup **10**

5 General performance of the 4A convection scheme **11**
5.1 Time-mean . . . 11
5.1.1 Zonal averages . . . 11
5.1.2 Single equatorial point . . . 13
5.2 Timestep by timestep behaviour . . . 17
5.2.1 Very large updraught mass-fluxes in mid-level and deep convection . . . 19
5.2.2 Intermittency of deep convection . . . 23
5.2.3 Early termination of deep convection . . . 25
5.2.4 Noise generated by forced detrainment . . . 27
5.2.5 Early termination of downdraughts . . . 28
5.2.6 Boundary layer mixing . . . 28
5.2.7 Mid-level convection acting as deep convection . . . 29
5.2.8 The role of deep convection in upper tropospheric humidity . . . 30
5.2.9 Balance between dynamics and physics . . . 31

6 Sensitivity to timestep of the 4A convection scheme. **35**
6.1 Time-mean . . . 35
6.1.1 Zonal averages . . . 35
6.1.2 Single equatorial point . . . 38
6.2 Timestep sensitivity of the temperature and moisture balance . . . 39

7 Conclusions **41**
7.1 General behaviour of the convection scheme . . . 41
7.1.1 Behaviour of mid-level convection . . . 41
7.1.2 Behaviour of deep convection . . . 41
7.1.3 Generic behaviour . . . 42
7.2 Timestep dependence . . . 42

8 Recommendations and future work **43**

The Tropical Behaviour of the Convective Parametrization in Aquaplanet Simulations and the Sensitivity to Timestep

Martin Willett and Sean Milton

18 January 2006

Abstract

The tropical performance of the Unified Model has for some time been recognised as an area that has the potential for improvement. The structure of temperature biases, humidity biases, and the precipitation errors visible in forecasts suggests that the convection scheme is at least partially responsible. The aquaplanet configuration was used to examine in detail the tropical behaviour of the UM and in particular the behaviour of the convection scheme. The aquaplanet proved to be a very useful methodology for this task because: there is a full interaction of physics and dynamics; it runs relatively quickly; it has a simple climate; a single gridpoint is reasonably representative of the aquaplanet's zonal mean, and hence it is easier to attribute potential errors to physical processes. By examining a wide range of diagnostics from a single equatorial point a number of deficiencies in convection scheme were identified and investigated. The balance between the physics and dynamics was also investigated. It was shown that the physics and dynamics are only in balance in terms of temperature and humidity on timescales greater than approximately 3-hours and 6-hours respectively. The model timestep was reduced to 15-minutes and 5-minutes in order to test the sensitivity of the convection scheme and the model in general and to understand how the identified deficiencies respond. Areas where the convection scheme could potentially be improved are given and and some specific improvements suggested. Suggestions for future work that should help to further improve the convection scheme are also made.

1 Introduction

There has been a persistent forecast error structure in the tropics since the introduction of a new operational NWP model (cycle G27) in August 2002. The tropical performance of the UM is discussed in detail in Milton *et al* (2003) and summarised in Section 2 of this report. The new UM introduced a new dynamical core and changes to many of the physics schemes. One of the major changes was the introduction of the 4A convection scheme. This is described in detail in UM documents Lock (2003) and Maidens (2005) and summarised in Section 3. The nature of the errors observed in the tropics suggests that the convection scheme is at least partially responsible. An idealised aquaplanet configuration of the UM was set up to study the behaviour of the convection scheme and of the model in general in the tropics. An aquaplanet was used because it has a simple zonally symmetric climate, and there is a full interaction of physics and dynamics unlike in a single column model. In addition, this work is principally concerned with the model's tropical oceanic behaviour and hence an aquaplanet is an ideal testbed. Section 4 describes the aquaplanet configuration of the UM. Section 5 describes the model's time-mean performance and it's behaviour on a timestep-by-timestep basis at a single point. Some characteristics of the model's behaviour are discussed. Section 6 describes how the model's tropical behaviour is affected by reducing the timestep. The conclusions are given in Section 7. The ultimate aim of this work is to identify areas of the current convection scheme or other parametrizations that could be improved and would lead to improvements in the UM's tropical performance. Recommendations for improvements and associated future work are given in Section 8.

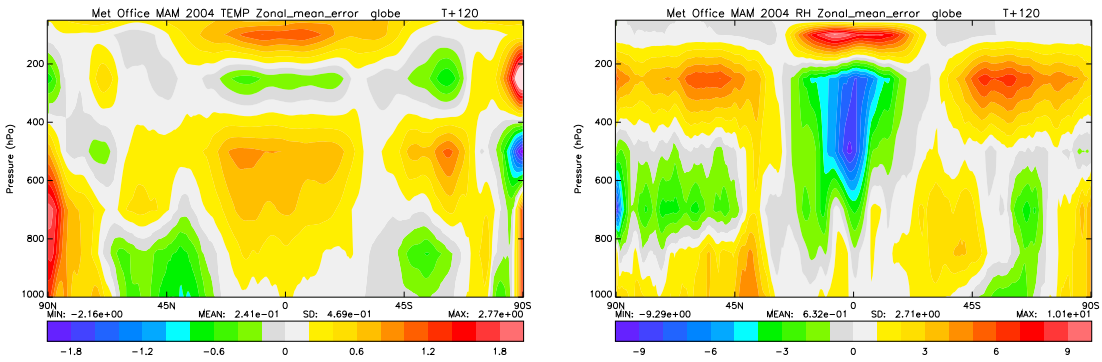

Figure 1: Zonal-mean error relative to analysis at T+120 in temperature (left) and relative humidity (right) for spring 2004.

2 Model systematic errors and relation to convection

There are systematic biases in forecast temperatures and humidities in the tropics (Fig 1). Throughout the mid-troposphere up to height of 350hPa there is a zonal-mean warm bias of up to 1K at T+120, and in the upper-troposphere there is a cold bias of up to 0.5K. There is also a dry bias throughout much of the free troposphere and a moist bias at the tropopause. In general, too much precipitation is forecast over the tropical oceans, especially in the Indian ocean and Eastern Pacific (Fig 2). Too little precipitation is forecast over continental land and over tropical islands such as Indonesia. Overall, too much precipitation is forecast in the tropics and globally. The excess precipitation over the Indian ocean is consistent with the excessive near-surface convergence and upper-level divergence forecast in this region (Fig 3). These errors are persistent across season and can be readily seen in individual forecasts. In addition, the observations show much greater variability in precipitation on timescales between 6 hours and several days than the model typically forecasts.

It is difficult to differentiate the cause and effects of this error structure because of the feedback processes involved, but a possible hypothesis for the growth of these errors is as follows. There is excessive convection in the Indian ocean area. This produces too much convective precipitation, heating and drying in that area. The excessive convective heating drives an over active Walker type circulation. The upward vertical flow over the Indian ocean is balanced by reduced upward or increased downward vertical flow over Indonesia and the tropical Pacific. The reduction in the upward flow over Indonesia suppresses the deep convective processes and results in reduced precipitation. Because of the excessive forcing over the Indian ocean the near-surface easterlies in the central eastern Pacific are too strong. This causes too much evaporation and hence too much precipitation in the ITCZ in the Pacific.

Evidence from a number of diagnostic studies suggests that the size of these errors in the large-scale flow and the precipitation may be reduced by reducing the strength of convection. Although reducing the strength of convection also reduces the warm bias in the mid-troposphere it also increases the cold-bias in the upper troposphere. This suggest that the dipole heating error arises from an error in the vertical distribution of heating and not just and an overall excess of heating.

3 Description of the 4A convection scheme

The 4A convection has three distinct types of convection, shallow, deep and mid-level convection, that are diagnosed and treated in different manners. However, all of them are based on the same Gregory and Rowntree (1990) mass-flux scheme. The convection scheme includes a treatment of updraughts, downdraughts, precipitation processes and convective momentum transport. This section gives a brief introduction to the scheme. For a fuller description see Maidens (2005). Emphasis is given to mid-level and deep convection because these are the dominant convection types in the deep tropics, and

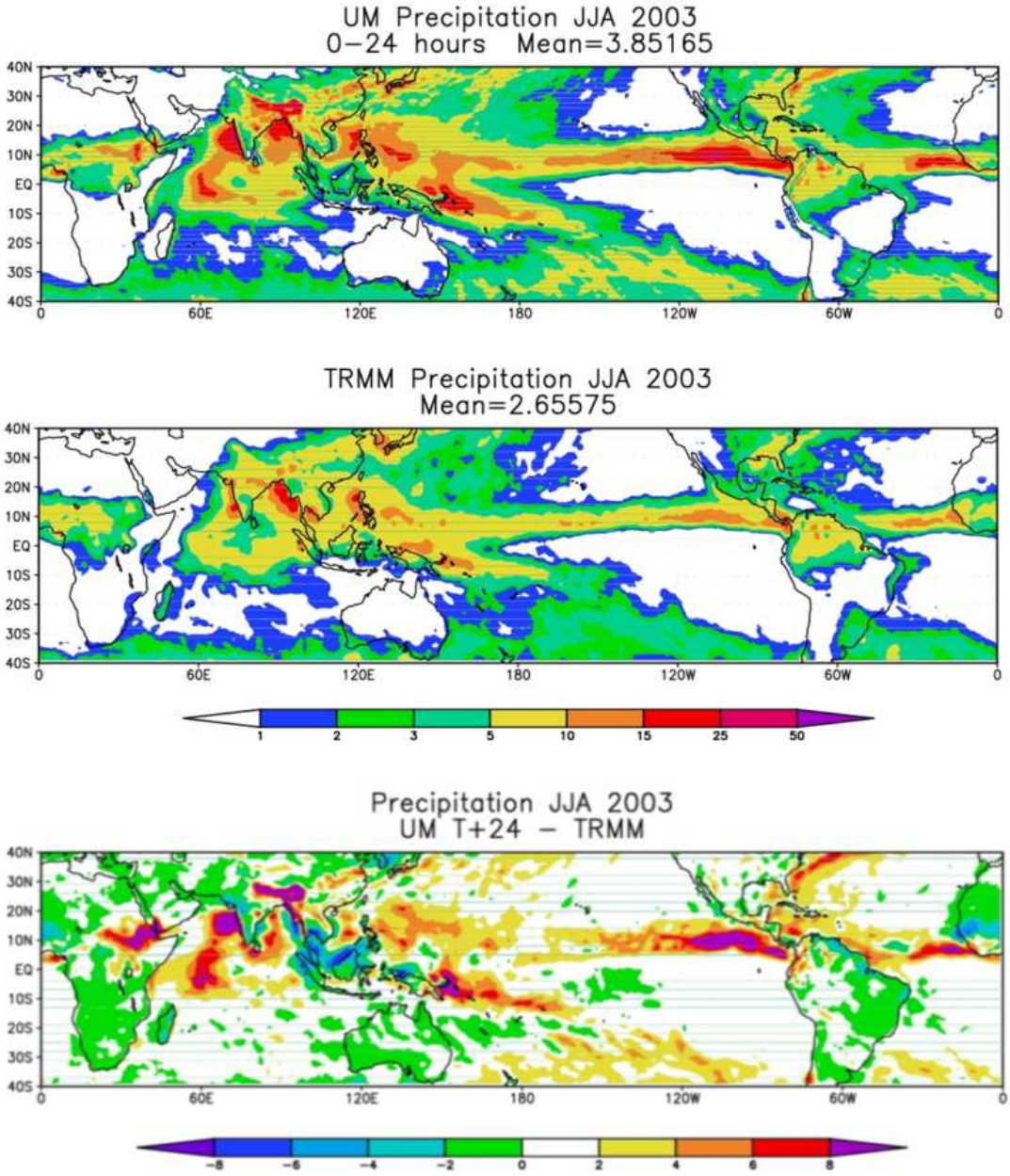

Figure 2: The mean tropical precipitation at T+24 from the operational UM in mm/day from Summer 2003 (top); the mean tropical precipitation from the TRMM for the same period (middle); and the difference in mm/day (bottom).

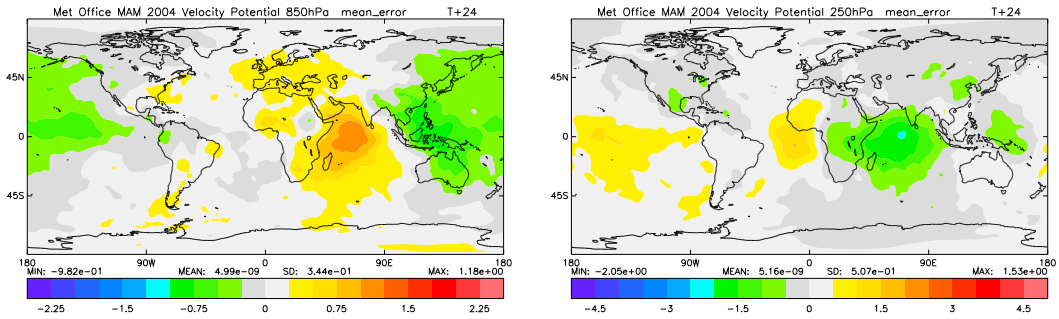

Figure 3: Error in velocity potential relative to analysis at T+24 at 850hPa (left) and 250hPa (right) for spring 2004. Positive values indicate excessive convergence and negative values indicate excessive divergence.

to the thermodynamic processes in the scheme; the convective momentum transport processes are not discussed. The essential components of any mass-flux convection scheme are the triggering and diagnosis of convection type, the treatment of updraughts and downdraughts, and the effects on the environment - these are described in the following sections.

3.1 Triggering and diagnosis of convection type

Shallow and deep convection are intended to represent surface driven convection and their diagnosis is intricately linked to the boundary layer (BL) scheme. The BL scheme explicity diagnoses seven different BL types (Lock (2003)). If shallow convection is diagnosed then the BL is diagnosed as either decoupled stratocumulus over cumulus (BL type V) or cumulus capped (BL type VI). If deep convection is diagnosed then the BL is cumulus capped. Shallow and deep convection are mutually exclusive. See Table 1.

Surface driven convection type\Boundary layer type	I	II	III	IV	V	VI	VII
Shallow convection					X	X	
Deep convection						X	
No surface driven convection	X	X	X	X			X

Table 1: Relationship between boundary layer type and surface driven convection type. An X indicates an allowable combination of BL type and surface driven convection type.

The diagnoses of deep and shallow convection are based on an undilute parcel ascent. The parcel ascent is only performed if the BL is classed as unstable, i.e. there is a positive buoyancy flux between the surface and model level (ML) 1. If the BL is stable then surface driven convection cannot occur.

A parcel is lifted from the surface layer (taken to be the ML just above 0.1 times the height of the surface mixed layer from the previous timestep). The parcel continues to ascend until it becomes slightly negatively buoyant. The small amount of negative buoyancy is dependent on the surface fluxes and the height of the surface mixed layer from the previous timestep and is typically $0.2K < \theta'_v \lesssim 1.0K$. Above the lifting condensation level (LCL), in addition to the buoyancy test, the ascent will also terminate at the level at which it has maximum buoyancy over the environment. This is done by identifying the layer at which the vertical gradient of the dry static energy in the environment is 25% greater than the gradient for the parcel.

Cumulus is then diagnosed if any of the the following conditions are met:

- The undilute adiabatic parcel ascent from the surface layer reaches at least the ML below the specified maximum number of BL levels. (The maximum number of BL levels is set to 13 with

the current vertical resolution and therefore the parcel must reach ML 12 which is at a height of 2880m with no orography).

- The magnitude of the gradient of the environmental total water content with respect to height in the cloudy levels is at least 10% greater than that in the subcloud levels. The subcloud gradient is calculated between the surface level and the LCL. The in-cloud gradient is calculated between the LCL and the lower of the ML reached by the parcel and the ML just below 2500m. This test is done to differentiate between cumulus capped BLs and stratocumulus capped BLs.

If cumulus is diagnosed then shallow convection is tested for. Shallow convection is diagnosed if the following conditions below are met otherwise the cumulus is assumed to be deep:

- There is a minimum in parcel buoyancy above the level where the parcel ascent would terminate.
- The height of this minimum is no higher than the terminating level plus 1.25 times the distance between the LCL and the terminating level.
- At this minimum the parcel buoyancy is less than 0.55*the parcel buoyancy at the terminating level.
- The large-scale vertical velocity at the highest specified BL level (i.e. ML 13 (~680hPa)) is negative.
- The parcel ascent terminated below the higher of 2.5km or the freezing level (~4.5km/~590hPa).

If these conditions are not met then deep convection is assumed by default. It should be noted that the parcel ascent is used to diagnose shallow and deep convection only and is not used to determine mass fluxes or convective increments. Either deep or shallow convection will then initiate from the ML just below the LCL. This level is designated NTML, i.e. the number of turbulently mixed levels.

The triggering of mid-level convection is very different to that of shallow or deep convection. It may trigger anywhere except where the BL scheme, shallow convection and deep convection are operating. Mid-level convection is allowed to occur on the same gridpoint at shallow or deep convection but only above where they have terminated. For mid-level convection to occur, the buoyancy relative to the environment of a parcel lifted to the next ML must exceed a critical threshold. The critical threshold is currently set to 0.2K.

3.2 Updraughts

3.2.1 Mass flux profile

In shallow, deep and mid-level convection, the convective updraught is modelled as a single cloudy plume that is intended to represent an ensemble of clouds (Gregory and Rowntree (1990)). The mass flux at cloud base is determined from the closure. The initial parcel properties are different for shallow, mid-level and deep convection and are described in Table 2. As the parcel ascends it interacts with the cloud free environment by entrainment, mixing detrainment and forced detrainment. Through these mechanisms the mass-flux is modified, i.e. $-\frac{\partial M}{\partial p} = \epsilon M - \mu M - \delta M$ where M is the mass flux, ϵ is the entrainment rate, μ is the mixing detrainment rate and δ is the forced detrainment rate. The ascent will continue until the conditions for termination are met.

Convection type	Initial potential temperature and specific humidity
Shallow	By solving $-0.17\overline{w'\theta'_{v0}} = -M_b\left(\theta^{Env}_{v,ntml+1} - \theta^{Env}_{v,ntml}\right) + M_b\left(\theta_{v,init} - \theta^{Env}_{v,ntml}\right)$ and $q_{init} = q_{sat}\left(\theta_{init}, p_{ntml}\right)$
Mid-level	$\theta_{init} = \theta_{start} + 0.2 * \min\left(\frac{\Delta p}{5000}, 1.0\right)$ and $q_{init} = q_{start}$
Deep	By solving $\theta_{v,init} - \theta^{Env}_{v,ntml} = -0.5\left(\theta^{Env}_{v,ntml+1} - \theta^{Env}_{v,ntml}\right) + 0.5$ and $q_{init} = q_{sat}\left(\theta_{init}, p_{ntml}\right)$

Table 2: The initial potential temperatures and specific humidities of a convective parcel. $\overline{w'\theta'_{v0}}$ is the surface virtual potential temperature flux, M_b is the cloud base mass flux, θ_v is the virtual potential temperature. The subscripts $init$, $ntml$, and $start$ refer to the initial parcel properties, the number of turbulently mixed levels, and the starting level of mid-level convection.

Entrainment is the movement of cloud free air into the cloudy plume. It increases the updraught mass-flux but also dilutes the parcel properties and hence reduces the parcel buoyancy. Entrainment occurs on every ML on which convection is occurring.

Detrainment is the movement of cloudy air from the plume into the environment. It reduces the updraught mass-flux and also modifies the large-scale environment. Mixing detrainment occurs on every ML on which convection is occurring. Forced detrainment only occurs when the buoyancy of the parcel falls below a critical value, $XSBMIN = 0.2 * MIN\left(\frac{\Delta p}{5000}, 1.0\right)$, which equates to about 0.1K near the LCL and the top of the troposphere, and about 0.16K in the mid troposphere. Forced detrainment always occurs where convection terminates but can also occur lower down in the convective plume. In addition to entrainment and detrainment, the parcel properties will also be modified by the phase changes of the water within the cloud.

3.2.2 Entrainment and detrainment rates

The same formulation of fractional entrainment and detrainment rates is used for mid-level and deep convection. Shallow convection has its own formulation.

For mid-level and deep convection the entrainment and mixing detrainment rates are $\epsilon = 3\,A_E\,\frac{p}{p_\star^2}$ and $\mu = \epsilon\left(1 - \frac{1}{A_E}\right)$ respectively. Both these quantities have units of Pa^{-1} and are the fraction of the mass flux entrained/detrained per unit height in terms of pressure. A_E is a constant set to 1.5 (except at ML 1 where it is set to 1.0). This means that the mixing detrainment rate is one-third of the entrainment rate, and hence in the absence of forced detrainment the mass flux will always increase with height.

Forced detrainment is triggered when the parcel buoyancy falls below the critical value, XSBMIN. The virtual potential temperature of the air that undergoes forced detrainment is set equal to that of the environment. The forced detrainment rate is set such that after forced detrainment the parcel is buoyant by XSBMIN, and the parcel continues upwards.

The entrainment rates for shallow convection are defined by Grant and Brown (1999) and are based on LES turbulence results. A major difference is that the mixing detrainment rate is larger than the entrainment rate, i.e. $\mu = 1.3\epsilon$, and hence the mass flux always decreases with height. Forced detrainment is also included with shallow convection but the threshold parcel buoyancy is set to the initial parcel buoyancy.

Entrainment and detrainment in this report are quoted in terms of the mass entrained/detrained within a ML, e.g. for entrainment $E = \epsilon\,\Delta p\,M$, where Δp is the pressure thickness of the model layer and M is the updraught mass flux. Like the mass flux, this form of entrainment and detrainment has units of Pas^{-1}.

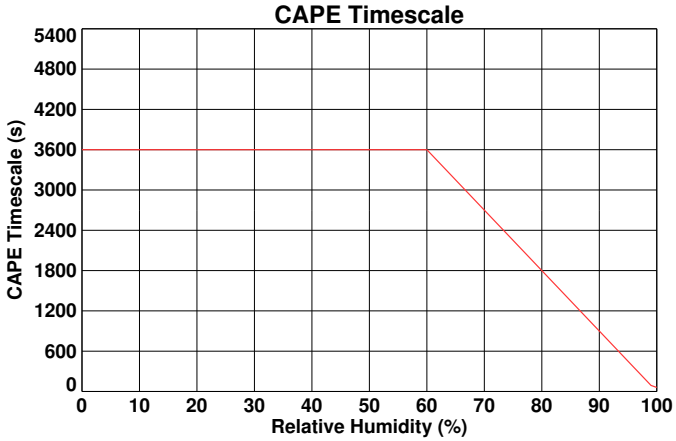

Figure 4: The CAPE timescale in seconds as a function of the mean relative humidity over the cloud environment.

3.2.3 Termination

The conditions for the termination of deep and mid-level convection are the same. The first condition that has to be met is that forced detrainment has to occur - see above. Convection will then terminate if at the next ML either: (i) the buoyancy of the parcel is greater than that of undilute parcel lifted from the level at which convection started (the buoyancy of the undilute parcel is calculated using the approximation in Maidens (2005)); or (ii) the mass flux (calculated using the reference mass flux M_{ref}[1]) falls below a small critical level which is typically $0.033 Pas^{-1}$. Termination will also be triggered when the parcel reaches the top of the model.

Shallow convection terminates at the maximum height of the undilute parcel ascent in the convection diagnosis routine.

3.2.4 Closure

Mid-level and deep convection both use the CAPE closure to determine the mass flux at cloud base. The cloud base mass flux is scaled such that the convective event would reduce the amount of CAPE to zero over the specified CAPE timescale, i.e. $M_{new} = M_{ref} \left(\frac{CAPE}{\frac{\partial CAPE}{\partial t}\big|_{ref} \tau} \right)$ where M_{new} is the CAPE scaled mass flux, M_{ref} is a reference mass flux, $\frac{\partial CAPE}{\partial t}\big|_{ref}$ is the rate of change of CAPE calculated using the reference mass flux, and τ is the CAPE timescale.

The CAPE timescale is set to one-hour. However, if the mean relative humidity of the cloud environment exceeds 60% then the timescale is reduced linearly such that the timescale would be zero at a relative humidity of 100%; the timescale is never allowed to be zero because a minimum timescale of 60s is imposed (Fig 4) .[2]

For reasons of numerical stability the mass flux at any level is not allowed to exceed the CFL limit. If a diagnosed mass flux does exceed the CFL limit, i.e. $M_k > \frac{\Delta p_k}{\Delta t}$ where $\Delta \mathrm{p}_k$ is the pressure thickness of the model layer and Δt is the convection timestep, then the mass fluxes are all rescaled such that the mass flux is equal to the CFL limit, i.e. $M_k = \frac{\Delta p_k}{\Delta t}$. Both the CAPE scaling and the CFL limit scaling are applied to the increments and precipitation rates calculated using M_{ref} .

The cloud base mass flux for shallow convection, M_b, is directly dependent on the mixed-layer convective velocity scale, $w_\star$, which is supplied by the boundary-layer scheme, i.e. $M_b = 0.03 w_\star$.

[1] M_{ref} is calculated using the buoyancy closure that was in operation prior to the CAPE closure.

[2] In January 2005 the operational forecast UM (cycle G34) was switched to a 30-minute CAPE timescale. The timescale is reduced linearly as a function of RH when the RH is greater than 80%.

3.2.5 Precipitation

The precipitation within the updraught is created by converting all the cloud liquid water in excess of a critical value to precipitation. This critical value is currently set to $MIN\left(0.001,\ 0.5q_{sat}^{Env}\right)kg/kg$. For shallow and mid-level convection precipitation is only created once the cloud depth exceeds 1.5km when over the sea or 4km when over land. This limit is reduced to 1km if the cloud reaches above the freezing level.

3.3 Downdraughts

3.3.1 Diagnosis

There are several conditions that the convective cloud must meet before the initiation of downdraughts is tested for. The cloud top pressure must be more than 150hPa from the surface, the depth of the cloud must exceed 150hPa, and the updraught must be saturated in the layer in which it terminates. If these conditions are met then each level is tested, starting from the cloud top and proceeding to within 150hPa of the surface, to see if it can initiate a downdraught. The initial potential temperature and humidity of the downdraught are taken to be an equal mix of the updraught and environmental properties. The downdraught air is then brought to saturation through the evaporation or sublimation of precipitation. A downdraught will then initiate if the parcel is negatively buoyant with respect to the environment.

3.3.2 Mass flux profile

Downdraughts are modelled as inverted updraughts but with only a single detrainment term, i.e. $\frac{\partial M^{DD}}{\partial p} = \epsilon^{DD}M^{DD} - \mu^{DD}M^{DD}$. Of course, the downdraught would soon become buoyant on descent through the adiabatic warming of the parcel. However, a proportion of the precipitation that is formed within the updraught is assumed to fall within the downdraught. The amount of precipitation that is transferred from the updraught into the downdraught is determined by assuming continuity of precipitation mixing ratio between the updraught and the downdraught. In the downdraught the precipitation evaporates or sublimates at the rates described by Gregory (1995). This evaporation cools the downdraught parcel and maintains its negative buoyancy. The unevaporated precipitation falls as precipitation at the surface if the downdraught reaches that far.

3.3.3 Entrainment and detrainment rates

The entrainment rate for downdraughts is constant with height, $\epsilon^{DD} = \frac{A_E C_{DD}}{p_\star}$, where $A_E = 1.5$ and $C_{DD} = 3.0$, except at the freezing level where the entrainment is enhanced by a factor of $MIN\left(1.8 * 10^{-6}\,\frac{M_{init}^{DD}}{C_{DD}p_\star},\ 6.0\right)$. The formulation of the downdraught detrainment rate is similar to that of the updraught mixing detrainment rate except for a dependence on the height relative to the freezing level. Above the freezing level the downdraught detrainment rate $\eta^{DD} = \frac{1}{C_{DD}}\epsilon^{DD}\left(1 - \frac{1}{A_E}\right)$ and below the $0^\circ C$ level $\eta^{DD} = \epsilon^{DD}\left(1 - \frac{1}{A_E}\right)$. Therefore, the detrainment rate is three times larger below the freezing level than it is above the freezing level. The enhancement factor that is applied to the entrainment is not applied to the detrainment. Within 100hPa of the surface the entrainment rate is set to zero and the detrainment rate is set such that the downdraught detrains its remaining mass evenly across the lowest 100hPa.

3.3.4 Termination

The downdraught will continue to descend until its buoyancy relative to the environment exceeds 0.5K. If the downdraught reaches to within 100hPa of the surface then no test for termination is performed, and the downdraught is detrained evenly across the lowest 100hPa.

3.3.5 Closure

The initial downdraught mass flux is simply taken to be proportional to the updraught mass flux at a reference height, i.e. $M_{init}^{DD} = \alpha M_{ref}^{UD}$. The constant $\alpha = 0.05$ and reference height is taken to be 3/4 of the way up the cloud. The initial mass flux of the downdraught is therefore independent of where the downdraught initiates.

3.4 Effects of convection on the environment

The updraughts affect the environment through the detrainment of cloudy air, the compensating environmental subsidence, the formation of the updraught and the evaporation of non-downdraught precipitation. The updraught mass-flux is balanced in the environment by compensating subsidence. This compensating subsidence will modify the environment through adiabatic heating and the transport of (usually) relatively dry air vertically downwards, i.e. the compensating subsidence will act to warm and dry the environment. Detrainment affects the environment in several ways. Detrainment will transport cloud condensate, which then evaporates in the dry environmental air, and water vapour from the plume to the environment. Hence, detrainment will always increase the humidity of the large-scale environment. The evaporation of the detrained cloud condensate will also cool the environment. The plume will usually be warmer than the environment, and therefore, the sensible heat from the mixing detrainment will tend to warm the environment. With forced detrainment, the virtual potential temperature of the detrained air is set equal to that of the environment but the detrained air is saturated. Therefore, the sensible heat from forced detrainment will tend to cool the environment. The subcloud layer is moistened and cooled by the evaporation of non-downdraught precipitation. The heat and moisture used to create the convective parcel's initial temperature and humidity perturbation is removed from the convective temperature and humidity increments at the ML at which convection initiated.

Downdraughts affect the environment through the detrainment of downdraught air, the compensating upward flow, and the formation of the downdraught. The downdraught mass-flux is balanced in the environment by a compensating upward flow. This flow will modify the environment by adiabatic cooling and the transport of relatively moist air vertically upwards, i.e. the upward flow will tend to cool and moisten the environment. In general, the detrainment of downdraught air will transport relatively cool and moist air into the environment and hence will cool and moisten the environment. However, near the surface the downdraught may be unsaturated and can act to dry the environment. The downdraught is formed by cooling and moistening the downdraught parcel. To compensate for this, the environment is warmed and dried at the level at which the downdraught is formed.

The final convection process that affects the environment is the mixing of the convective increments from the lowest ML up to the number of turbulently mixed levels, NTML. The effects of this are discussed in Section 5.2.6.

Table 6 in the Appendix identifies the different convective processes in the convection scheme and quantifies their contribution to the temperature and humidity increments.

4 Aquaplanet configuration and model setup

The aquaplanet configuration of the UM follows the set up in Neale and Hoskins (2000). The SST is symmetric with a single peak on the equator and fixed in time. An eternal equinox is imposed on the model such that the incoming solar radiation at the top of the atmosphere is also symmetric about the equator. A resolution of N48 is used which is equivalent to a gridbox of 415km*550km on the equator. The standard 38 ML set is used. Explicit diffusion and targeted diffusion, which is used to control gridpoint storms, are switched off. In the operational NWP model and climate versions of the UM two and three convection substeps respectively are done. However, in these experiments only one convection substep per model timestep was performed to give a clearer picture of the behaviour of the convection scheme.

The model was run from a start dump that had been spun up for 65 days using an aquaplanet configuration. The model was run for 40 days with a 30-minute timestep. In addition, the model was run with 15-minute and 5-minute timesteps to test the sensitivity to timestep. All 40 days of data were used in the analysis.

5 General performance of the 4A convection scheme

5.1 Time-mean

5.1.1 Zonal averages

The zonal- and time-mean updraught mass flux from the convection scheme is shown in Fig 5. There is a deep convective region within approximately 7° either side of the equator that reaches to about ML 27 (~140hPa - see Table 5 in Appendix). This is flanked by shallow convective regions that extend to approximately 22° either side of the equator and reach approximately ML 10 (~800hPa). A closer inspection of the updraught mass flux on the equator shows that it does not vary smoothly with height but has several peaks in its profile (Fig 6). One peak is at ML 14/15 (~640-590hPa) and another at ML 24 (~230hPa); there is also an inflection in the updraught mass flux at ML 5 (~950hPa). All these peaks correspond to peaks in the forced detrainment (although not shown separately the forced detrainment is the dominant detrainment term. The mixing detrainment will be one-third the magnitude of the entrainment but is of opposite sign). The peak at ML 5 is at or just above the LCL, the peak at ML 15 corresponds to the freezing level, and the peak at ML 24 lies just below the tropopause.

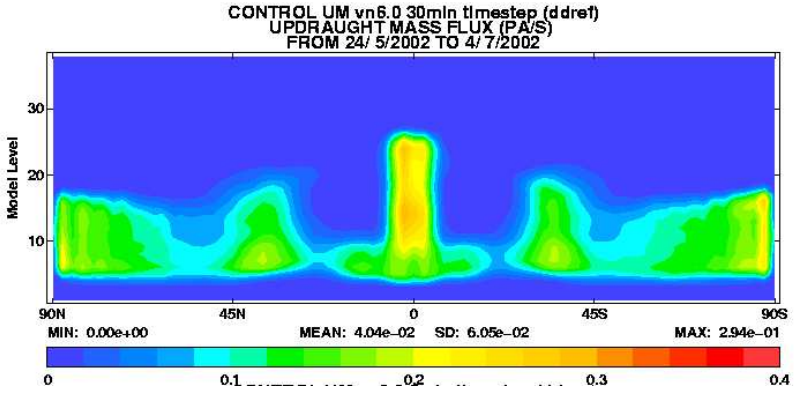

Figure 5: Zonal- and time-mean updraught mass flux (Pa/s).

The magnitude of zonal- and time-mean downdraught mass flux is smaller than the updraught mass flux; the peak value of the downdraught mass flux is approximately one-fifth as large as the peak updraught mass flux (Fig 6). However, most of the downdraught detrainment occurs below ML 6 and provides an important feedback between the convection scheme and the BL.

The zonal- and time-mean convective heating on the equator is also shown in Fig 6. There are two distinct peaks in the convective heating of about 7.5K/day at ML 12 (~720hPa) and at ML 16 (~550hPa). In between these maxima at ML 14 there is a minimum of ~6.5K/day. The dominant balance in the equatorial free troposphere is between the convective warming and the advective (adiabatic) cooling. Therefore, there is a minimum in the advective cooling at ML 14 reflecting the minimum in convective warming at this level. A minimum is also visible in the vertical wind velocity at this level (not shown). In the zonal- and time-mean meridional velocity field (Fig 7) the expected areas of convergence near the surface and divergence at the top of the troposphere associated with the Hadley circulation are clearly visible. However, there are also areas of weak divergence/convergence at 700hPa and 400hPa respectively that are also seen in the full model. This behaviour is consistent with the twin peaks in the convective heating that are subsequently reflected in the advective cooling and vertical wind velocities.

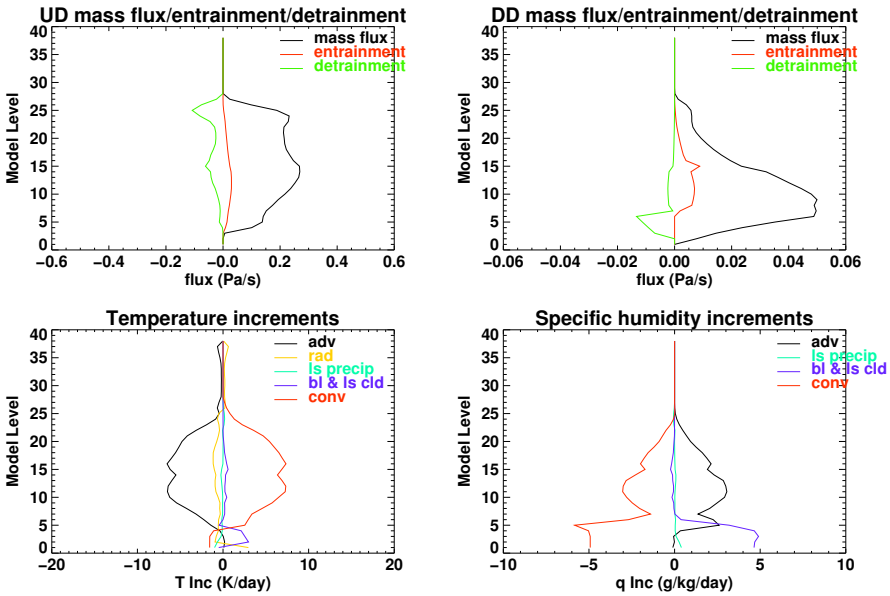

Figure 6: Profiles of zonal- and time-mean equatorial updraught massflux, entrainment and detrainment (top left); downdraught massflux, entrainment and detrainment (top right); thermal balance (temperature increments) in K/day (bottom left); and moisture balance (humidity increments) in g/kg/day (bottom right). Please note that the updraught and downdraught profiles have different scales on the x-axis.

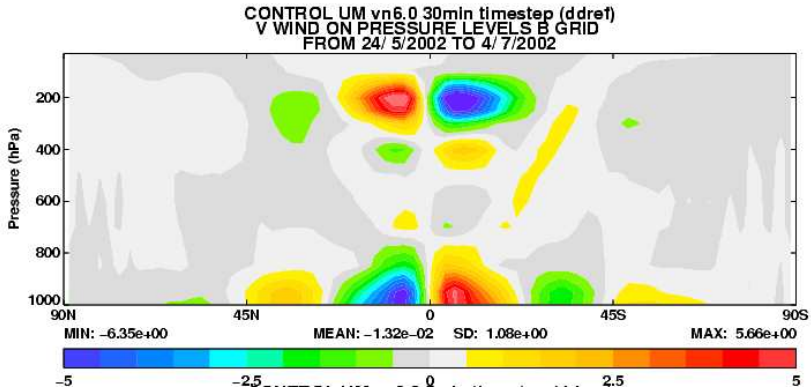

Figure 7: Zonal- and time-mean meridional wind.

Convection type	Frequency		
Shallow only	14.1	14.9	14.1
Shallow + Mid-level	0.8		18.4
Mid-level with BL type III	16.8	16.8	
Mid-level with BL types I, II, IV or VII	0.0		
Deep + Mid-level	0.8	24.1	
Deep only	23.3		23.3
Total convection	55.8		

Table 3: Frequency of convection type and combinations of convection type at the single equatorial point (percentage of total timesteps). (E.g. Shallow convection occurs on its own 14.1% of timesteps, with mid-level on 0.8% of timesteps, and hence in total on 14.9% of timesteps.)

The zonal- and time-mean humidity increments on the equator area also shown in Fig 6. In the free troposphere, above ML 5, there is a balance between the convective drying and the advective moistening. Below ML 5 the balance is between the convective drying and the moistening due to the BL and the advection. At ML 5, where the advective and BL moistening are both large there is a spike in the convective drying. At ML 15 there is a distinct local minimum in the convective drying and the advective moistening. These vertical structure of the temperature and humidity increments are discussed further in Section 5.1.2.

5.1.2 Single equatorial point

By looking at a single gridpoint and outputting the data at each timestep, it is possible to study the behaviour of the the model, and in particular the convection scheme, in much more detail. This has been done for a single point on the equator making it possible to identify the individual components responsible for the zonal- and time-mean fluxes and increments.

The equatorial zonal- and time-mean diagnostics (Fig 6) and the same time-mean diagnostics from the single equatorial point (not shown) are very similar. Therefore, the single point is considered to be reasonably representative of the behaviour of the model in the deep tropics, when averaged over this forty day period.

Frequency of convection Table 3 shows the frequency of convection subdivided by convection type and combinations of convection type (e.g. when mid-level convection occurs above shallow convection). Deep convection occurs on 24.1% of timesteps, mid-level convection on 18.4% and shallow convection on 14.9%. In total convection of some form occurs on 55.8% of timesteps. There are a small number of occasions when mid-level convection occurs above deep or shallow convection.

Updraughts. In Fig 8, the updraught mass flux has been subdivided into shallow convection, deep convection, mid-level convection with a well-mixed BL and mid-level convection with the remaining BL types (I, II, IV or VII). Deep convection is the largest contributing factor to the updraught mass flux. Mid-level convection with a well-mixed BL has a contribution of approximately half that of deep convection. Both deep convection and mid-level convection have two peaks but the mid-level has its peaks one or two MLs above those of deep convection.

There is a small contribution to the updraught mass flux from the shallow convection - the peak value is approximately 10% that of deep convection. When shallow convection has been diagnosed there is also a contribution to the UD mass-flux between MLs 20 and 27 (~140hPa), which is well above the level at which the shallow convection scheme operates. This is the mid-level scheme being triggered above the shallow convection region. There is no contribution from mid-level convection in conjunction with the other BL types.

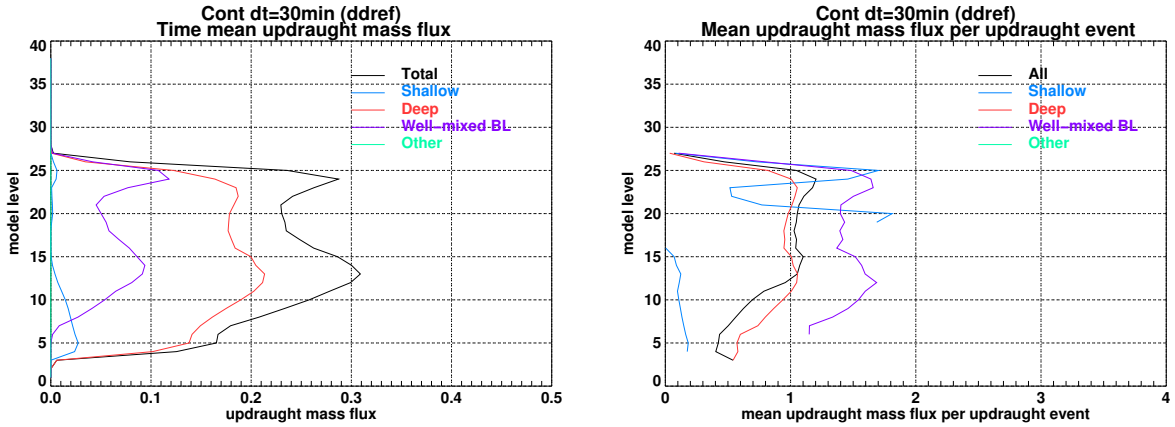

Figure 8: Vertical profiles of the time-mean updraught mass flux (left) and of the mean updraught mass flux per updraught event (see text for explanation) (right) at the single equatorial point. Both diagnostics are in Pa/s and are subdivided by convection type .

Fig 8 also shows the updraught mass flux meaned per updraught event. For example, the deep convection mean is the mean updraught only over the timesteps where deep convection is occurring. Similarly, the well-mixed mean is the mean updraught over the timesteps when the BL is well-mixed and the updraught mass flux is non zero (i.e. convection is occurring).The updraught mass flux when the BL is well-mixed is typically larger than the updraught mass flux of deep convection. The typical mass flux profile of a shallow convective event is much smaller than either deep or mid-level convection.

Fig 9 shows the frequency at which the updraughts are initiated and terminated. Shallow convection is initiated at the either ML 4 or 5 (~965hPa); deep convection is initiated at MLs 3, 4, or 5. As expected the shallow convection terminates between MLs 10 (~800hPa) and 15 (~580hPa). Deep convection can terminate anywhere above ML 13 but the large majority of deep convecting events terminate in the upper troposphere between ML 22 (~300hPa) and ML 28 (~115hPa). There is a small peak in the frequency of deep convection termination around MLs 15 and 16 that is probably related to the buoyancy minimum around the freezing level (typically ML 15). Surprisingly, a significant proportion of deep convecting events (~4% of timesteps which equates to ~17% of deep convective events) terminate at MLs 5 and 6 which is only one or two levels above their initiation level. This is discussed in more detail in Section 5.2.3. The contributions from shallow and deep convection to the frequency of updraught initiation above the LCL are very small but non-zero. This is due to mid-level convection operating above shallow or deep convection. Mid-level convection is permitted to operate at any level above the BL, and the frequency at which mid-level convection initiates is fairly constant between ML 7 and ML 20. However, there is a large peak in the frequency of the initiation of mid-level convection in the upper troposphere between ML 21 and ML 25 which is not fully understood. There is a peak in the frequency of termination of mid-level convection just above the freezing level, and again in the upper troposphere.

The mean updraught depth per updraught event as a function of the ML at which the updraught initiated is shown in Fig 10. The depth of the deep convection is very sensitive to the ML at which it initiates. If it initiates at ML 3 then it is about 24 MLs deep on average. However, if it initiates at ML 5 then it will only be about 10 MLs deep on average. It should be noted that these averages may not represent the depth typically reached by deep convection because the distribution of depths is likely to be bimodal because some deep convective events terminates after only a few levels. The sensitivity of the depth of deep convection to the initiating ML, which is defined by the diagnosed LCL, would imply that the behaviour of the deep convection is very sensitive to the diagnosis of the LCL. On average, the depth of shallow convection is about 8 MLs. For mid-level convection, there is a general reduction in updraught depth with initiation level, which is to be expected if convection is capped at the tropopause.

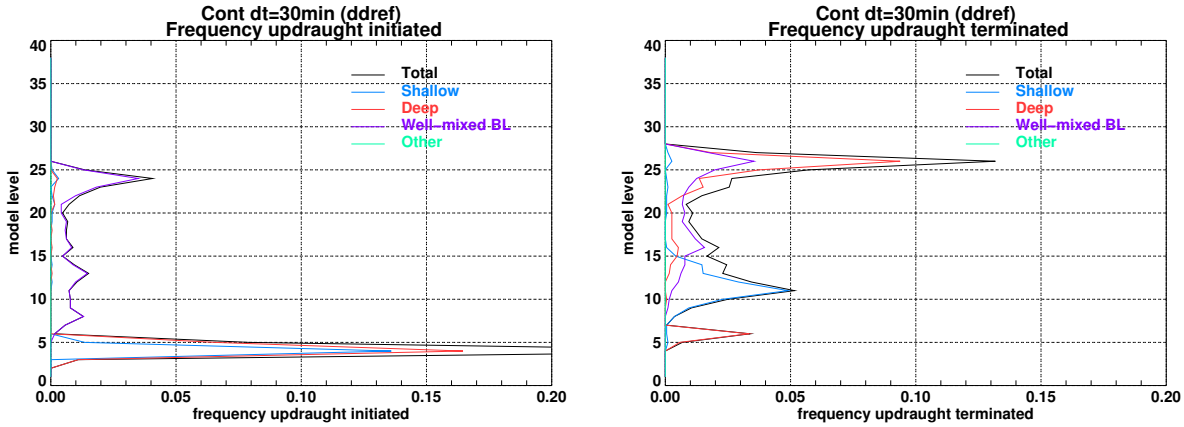

Figure 9: Frequency at which updraughts are initiated (left) and terminated (right). The values are the proportion of all timesteps that have updraughts initiating or terminating from the specified level.

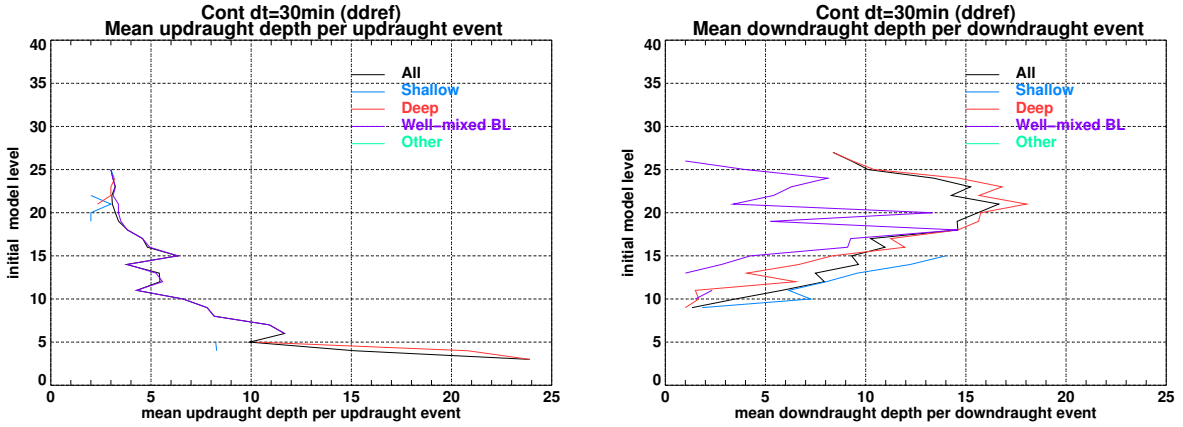

Figure 10: Mean updraught (left) and downdraught (right) depth in model levels as a function of initial model level.

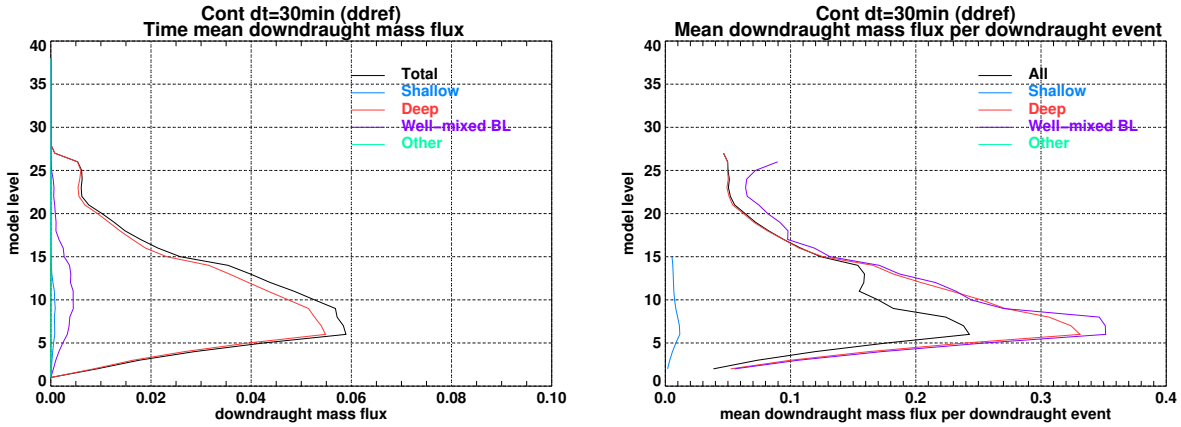

Figure 11: Vertical profiles of the time-mean downdraught mass flux (left) and the downdraught mass flux per downdraught event (see text for explanation) (right). Both diagnostics are in Pa/s and subdivided by convection type.

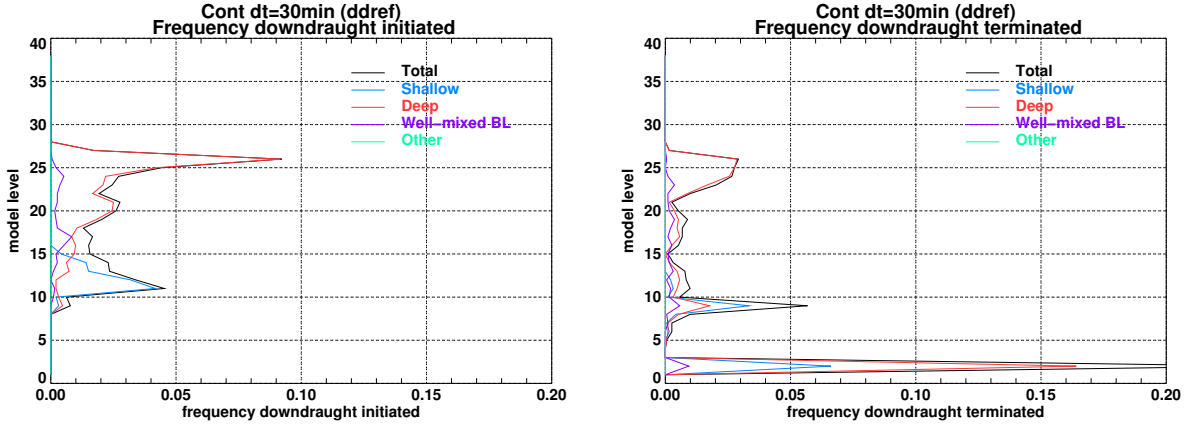

Figure 12: Frequency at which downdraughts are initiated (left) and terminated (right). The values are the proportion of all timesteps that have downdraughts initiating or terminating at the specified level.

Downdraughts. The structure of the time-mean downdraught mass flux for the single point (Fig 11) is very similar to that of the zonal-and time-mean (Fig 6). The downdraught mass flux starts at about ML 26 (~165hPa) and gradually increases until it reaches a peak between ML 9 and ML 6 (~840-930hPa). It then falls off to zero at ML 1. Deep convection is the dominant factor contributing to the time-mean downdraught mass flux. The contribution from the mid-level convection in the well-mixed BL is about 10% that of deep convection. With mid-level convection, the profile of downdraught mass flux is a similar shape but the peak occurs at about ML 10. If the downdraught mass flux per downdraught event is considered (Fig 11), it can be seen that a typical downdraught mass flux profile is similar in shape and magnitude in both the deep convection and mid-level cases. The time-mean contribution from shallow convection is much smaller than both the well-mixed BL and the deep convection. The typical mass flux is also much smaller and it is only non-zero below ML 15.

Deep convection downdraughts are initiated anywhere between ML 28 (~115hPa) and ML 8 (~870hPa) but there is a peak in the frequency at MLs 25 (~195hPa) and 26 (~165hPa) (Fig 12). There is no large peak in the frequency of mid-level convection downdraught initiation in the upper troposphere probably because the depth of mid-level convection updraught is insufficient to initiate downdraughts. Below ML 17 (~450hPa) the frequency of downdraught initiation for mid-level convection and deep convection are both small. Shallow convection downdraughts are initiated between MLs 15 (~580hPa) and 9 (~810hPa).

There are prominent peaks in the frequency of the termination of deep convection downdraughts between ML 24 and ML 26, at ML 9 (~810hPa) and at ML 2 (Fig 12). The peak in termination frequency in the upper troposphere indicate that many downdraughts terminate almost immediately (52% of downdraughts that start above ML 21 terminate before reaching ML 21) . The peaks in downdraught termination frequency at ML 9 and ML 2 are also seen in the shallow convection downdraughts and the well-mixed BL downdraughts. The peak at ML 2 is to be expected because if the downdraught penetrates to within 100hPa of the surface then the downdraught is forced to detrain evenly across the lowest 100hPa. The proportion of all downdraughts terminating at ML 9 is equal to about 25% of those that reach the surface. This peak in downdraught termination is discussed further in Section 5.2.5. The downdraughts may play a key role in the controlling oceanic tropical convection (Raymond, 1995), and therefore, the spurious early termination of downdraughts is likely to be significant.

On average deep convective downdraughts span a greater depth of the troposphere than mid-level convection downdraughts (Fig 10). The depth of deep convective downdraughts is very sensitive to the ML at which they are initiated with the deepest on average starting from ML 21. Above ML 21 the mean depth of the downdraught reduces dramatically - a downdraught initiated at ML 21 will be about 18 MLs deep on average, whereas a downdraught initiated from ML 25 will be only about 10 MLs deep.

Environmental effects Deep convection is the dominant convection type in the time-mean convective heating above the LCL (typically around ML 4 or 5) and cooling below the LCL (Fig 13). Deep convection is also the source of the minimum in the total convective heating at ML 14 (cf Fig 6). The minimum occurs one ML below the freezing level and therefore the melting of snow is the most likely source of this minimum. This is consistent with the minimum not appearing in the mid-level convective increments because mid-level convection tends to extend over only a few model layers and hence is too thin to produce precipitation (mid-level convection needs to be 1.5km thick at a sea point to produce precipitation).

Deep convection is also the dominant convection type in the time-mean convective drying. At the LCL and above, the major factor in the convective drying is the updraught compensating subsidence. The minimum in the convective drying around the freezing level and the small convective moistening in the upper troposphere is due to the forced detrainment of cloudy air which is at a maximum at these levels (Fig 6). The peak in the convective drying around the LCL is due to the peak in the environmental vertical gradient of humidity around this level (Fig 14) and the environmental drying that compensates for the process of bringing the initial parcel humidity to saturation. The minimum in the drying at ML 7 is caused by a combination of a relatively small environmental vertical gradient of humidity and a small updraught mass flux.

Both the temperature and humidity increments are fairly constant below ML5 because of the mixing of the convective increments. The mixing is also the source of the small (~1.0K/day) shallow convective warming below the LCL (see Section 5.2.6).

Mid-level convection has only a very small contribution to the time-mean temperature and humidity increments above the freezing level despite the time-mean mass-fluxes being between 25% and 50% of those of the deep convection. Much of the mid-level mass flux at these levels will initiate and terminate there and will be quite shallow. Therefore, the effects of compensating subsidence and detrainment will partially cancel out over time. Below the freezing level mid-level convection tends to be deeper and hence its effects are more consistent with deep convection.

5.2 Timestep by timestep behaviour

A good way to understand the behaviour of the convection scheme is to study the behaviour at single point timestep by timestep. Detailed diagnostics from a single point on the equator were output from the 40-day run. For each timestep the set of diagnostics defined in the appendix was plotted. An example of a shallow convective event is shown in Fig 15. The event occurs during a relatively suppressed period, which can be seen from the timeseries of precipitation. There is no large inversion limiting the vertical extent of the convection (see the tephigram or the buoyancy profile) but there is negative large-scale

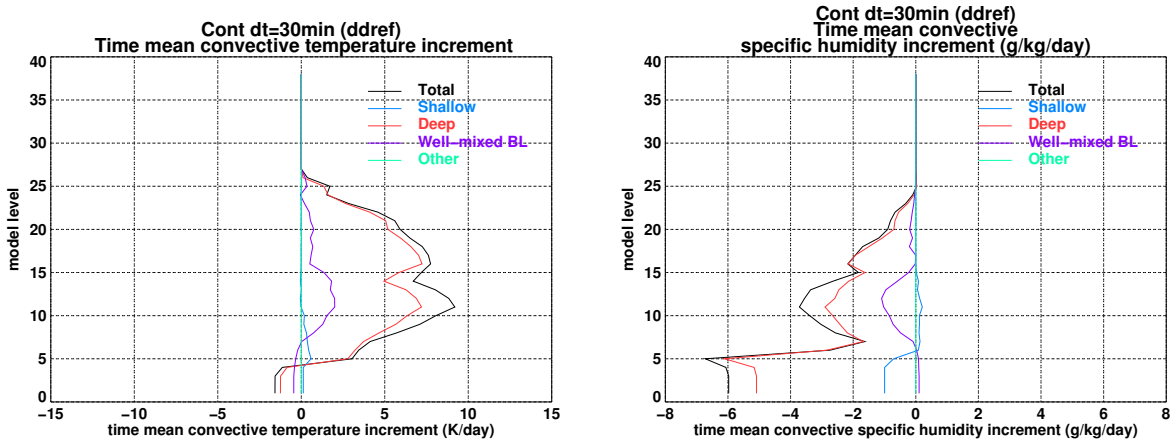

Figure 13: Mean convective temperature increments (left) and humidity increments (right) subdivided by convection type.

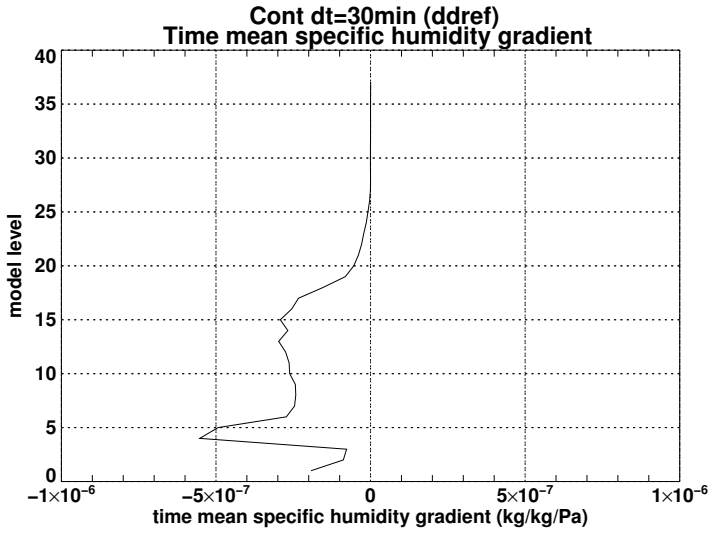

Figure 14: Vertical profile of the time-mean specific humidity vertical gradient with respect to pressure (kg/kg/Pa).

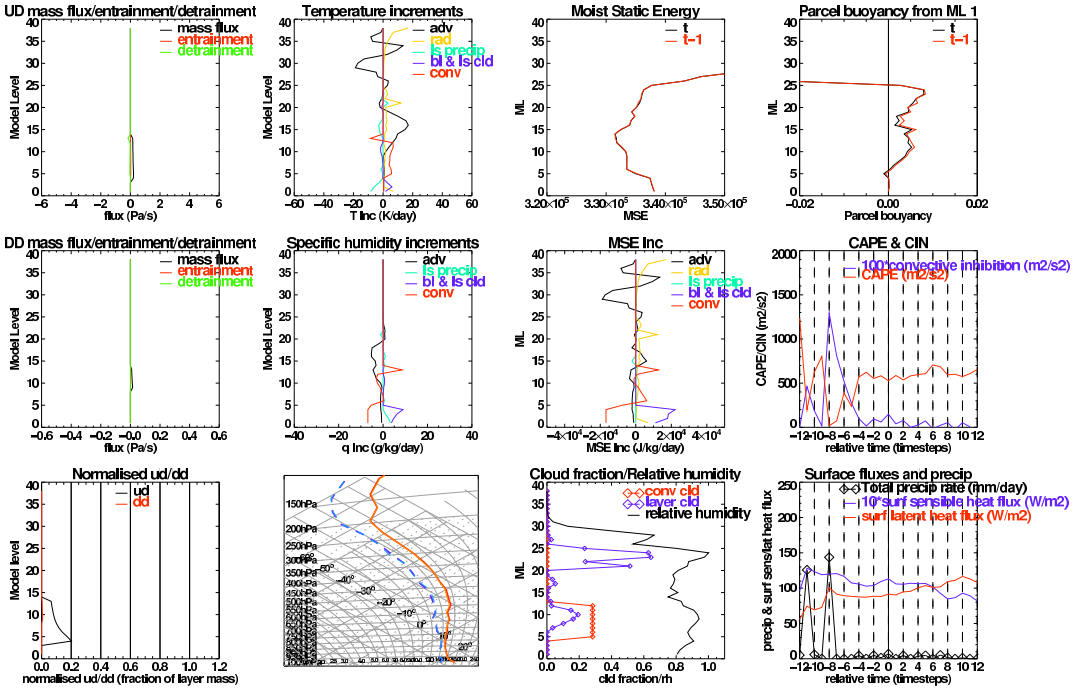

Figure 15: Shallow convection example at the single equatorial point.

vertical velocity around the freezing level (see the temperature increments). Convection starts just above the surface at ML 4 and terminates a few MLs below the freezing level at ML 13. The mass flux profile reduces with height as would be expected from the formulation of entrainment/detrainment rates (Section 3.2). A downdraught is formed but quickly terminates and a small amount of precipitation is produced.

An example of a pair of mid-level convective events is shown in Fig 16. They occur during a more active period when the large-scale vertical velocity is positive throughout the free troposphere. Both events convect over a relatively small depth which possibly explains why no downdraughts are initiated. The mass flux profiles increase with height as would be expected. Precipitation is produced, probably by the lower event, at a rate of about 25mm/day.

An example of a deep convective event is shown in Fig 17. Again the event occurs during an active period with positive large-scale vertical velocities throughout the free troposphere. A number of downdraughts are initiated but all of them terminate after only a few levels. Deep convection starts near the surface at ML 4, the mass flux profile increases with height and then convection terminates in the upper troposphere at ML 24. The deep convective event generates a large amount of precipitation at a rate of 150mm/day.

All the examples have been selected because they are typical events not because they are the most extreme. The remainder of this section describes some specific issues with the behaviour of the convective parametrization visible in these examples and in other events.

5.2.1 Very large updraught mass-fluxes in mid-level and deep convection

The updraught mass fluxes in the case of mid-level and deep convection are frequently very large - e.g. see the mid-level convection events in Fig 16 and the deep convective event in Fig 17. These large mass fluxes produce very large temperature, moisture and momentum (not shown) increments.

In the mid-level convection example shown, the maximum temperature increment is approximately 120K/day or about 2.4K in a single 30 minute timestep. This is unrealistically large especially when it is considered that this increment applies to a gridbox of dimensions 415km*550km*0.6km. The initial temperature profile closely follows a moist adiabat (except for a convective inhibition around the LCL

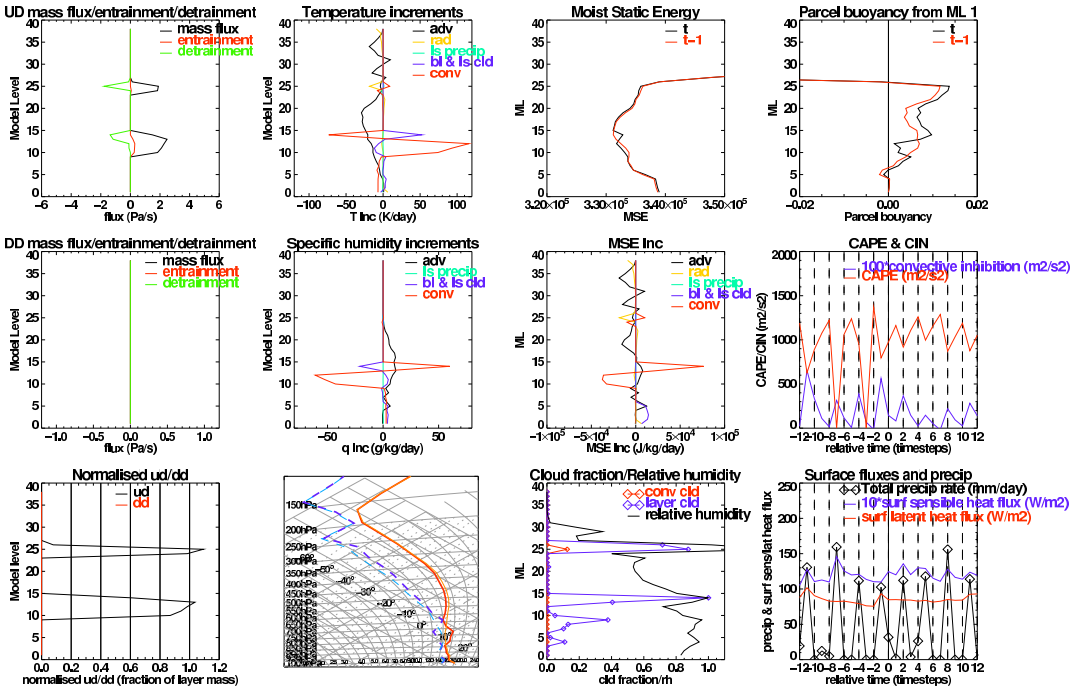

Figure 16: Example of mid-level convection at the single equatorial point.

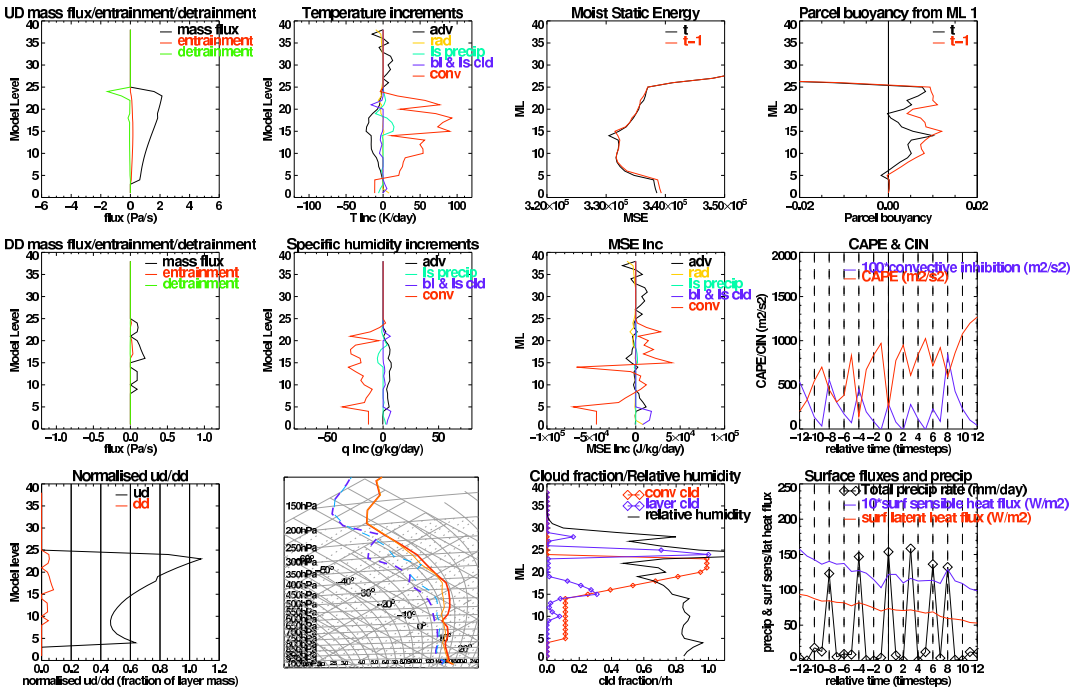

Figure 17: Deep convection example at the single equatorial point.

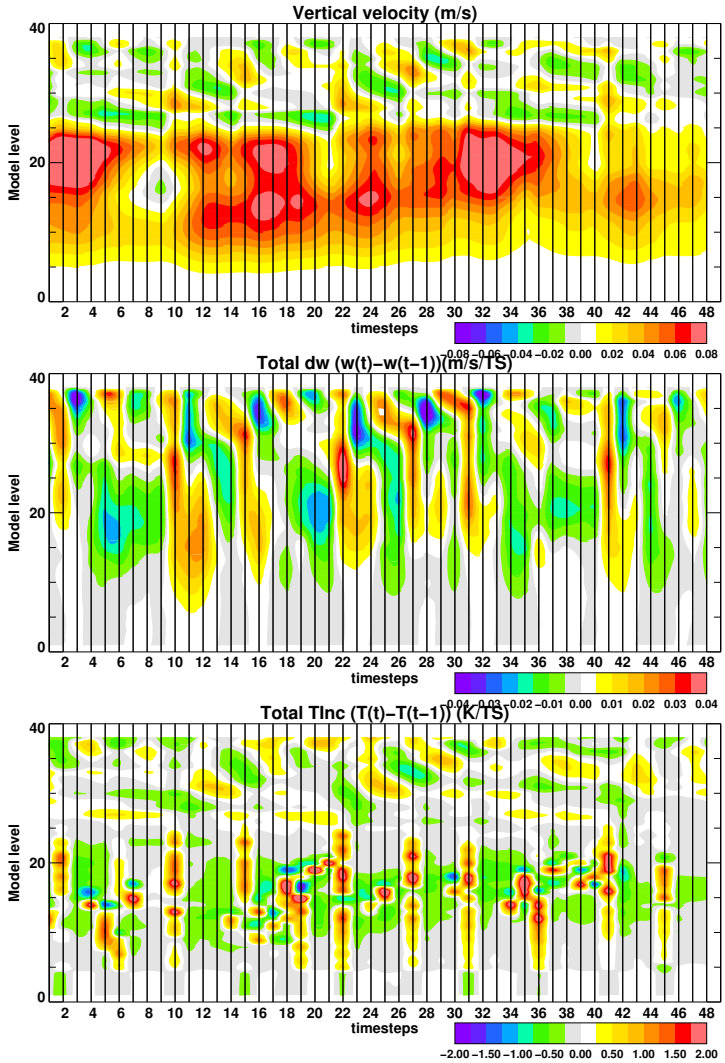

Figure 18: Time series of large-scale vertical velocity in m/s (top), vertical velocity increment in m/s/timestep (middle), and total temperature increment in K/timestep (bottom).

that inhibits the formation of deep convection - discussed further in Section 5.2.2) but the mid-level convection warms the environment to produce a large positive departure from a moist adiabat between 850hPa and 650hPa. This appears to be a common effect of mid-level convection when operating over a small number of layers.

In the deep convection example, the maximum temperature increment is about 2.0K in a single 30 minute timestep. Again this is unrealistically large. However, deep convection does in general appear to remove instabilities and smooth out the thermodynamic profile. Such large increments as these can lead to large imbalances between the physics and the dynamics on short timescales (discussed further in Section 5.2.9) and can also generate gravity waves in the stratosphere. Fig 18 shows a timeseries of vertical velocities, vertical velocity increments, and total temperature increments. The columns of strong tropospheric warming are deep convective events, the stronger of which (e.g. timesteps 10 and 22) generate gravity waves that propagate up through the stratosphere. It is not known if these gravity waves have a detrimental impact on the forecast performance.

The normalised mass flux is shown in Fig 15, Fig 16 and Fig 17. In the shallow convection example the maximum normalised updraught mass flux is about 0.2, i.e. the mass flux integrated over the timestep is 20% of the mass of model layer. However, the normalised mass fluxes of the mid-level and deep

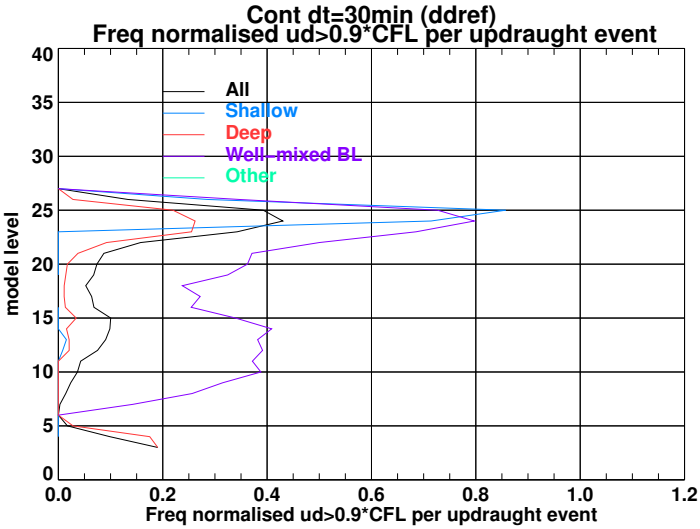

Figure 19: Frequency at which the updraught mass flux exceeds 90% of the CFL limit.

convection examples both reach (or just exceed[3]) 1.0. This implies that they are on their CFL limit. In the convection scheme the updraught mass-flux is checked after the CAPE scaling to determine whether it is exceeding the CFL limit, i.e. the mass flux integrated over the timestep is greater than the mass of the layer. If it is exceeding the CFL limit then the updraught mass-flux is reduced to the CFL limit and the increments scaled accordingly.

There is no diagnostic directly available to indicate if the mass flux has been reduced because it exceeded the CFL limit. Therefore, the frequency at which the normalised mass flux exceeds 0.9 was used as a proxy to quantify the extent to which the CFL limit is being reached on a particular level. This is shown as a function of ML for each convection type in Fig 19. In total 38.0% of deep convective events reach the CFL limit at one or more MLs. Deep convection most frequently hits the CFL limit near the top of the troposphere (up to 25% of the time on any particular level). A typical example of one of these occurrences can be see in the deep convection example in Fig 17. The CFL limit is also approached or exceeded up to 20% of the time at around the initiating ML and up to 3% of the time around the freezing level. An example of the deep convection updraught mass flux reaching or approaching the CFL limit at both the initiation level and near the freezing level may be seen in Fig 20. If there is no forced detrainment until the deep convective updraught terminates in the upper troposphere then the maximum normalised mass fluxes will always be at the terminating level. This is due to a combination of the vertical grid spacing and the entrainment and detrainment rates.

In total 89.2% of mid-level convective events reach the CFL limit at one or more MLs. Like deep convection, the CFL limit is most frequently reached in the upper troposphere, where the limit is reached up to 80% of the time, but it is also reached up to 40% of the time in the lower to mid troposphere.

In the case of mid-level convection operating over only a small number of levels in the mid- or upper-troposphere, three factors combine to generate the very large mass fluxes. Firstly, there is a small positive perturbation applied to the parcel's temperature at the start of the updraught calculation. This perturbation generates a small amount of additional CAPE that is not actually present in the environment. The perturbation generated CAPE is insignificant when there is significant amount of real environmental CAPE, however, in this case it is the perturbation that provides most or all of the parcel's CAPE. Secondly, in the upper troposphere, the environment is close enough to dry adiabatic that the rate of change of CAPE due to the parcel's ascent will be very small. Thirdly, the CAPE timescale is a relatively short one-hour and may be much shorter if the relative humidity is high. The factor used to scale the reference

[3]The normalised mass fluxes in the examples can be slightly larger than 1.0 because of approximations made the in the diagnostic calculation of the pressure thickness of model layers.

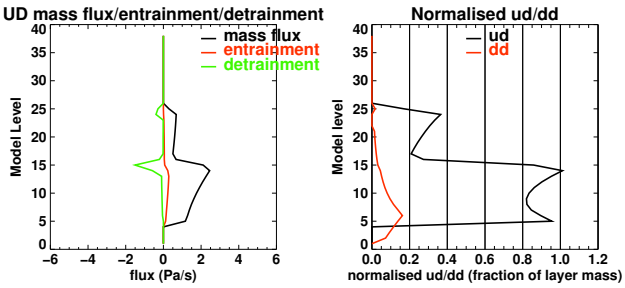

Figure 20: The updraught mass flux reaching or exceeding the CFL in the mid-troposphere (left) with it's associated normalised mass flux (right).

mass flux is $\frac{CAPE}{\frac{\partial CAPE}{\partial t}\Big|_{ref}\tau}$. Therefore, if the CAPE is relatively large, the rate of change of CAPE is small and the CAPE timescale is small then the scaling applied to the reference mass flux is very large.

In the case of deep convection, the intermittency in the triggering (Section 5.2.2) allows the environmental CAPE to build up in between events. The large amount of environmental CAPE and the relatively short CAPE timescale combine to generate large mass fluxes.

The CFL limit being exceeded can potentially have a number of adverse consequences.

- The CAPE closure is designed to reduce the CAPE to zero over the CAPE timescale, i.e. one-hour in this case. If the mass flux is limited to the CFL limit then it will not be enough to reduce the CAPE to zero over the CAPE timescale. Therefore, after convection a relatively large instability may remain in the thermodynamic profile. The large-scale dynamics can then act to try to remove this instability. This is a problem because it may potentially result in a gridpoint storm.

- The mass flux is limited to exactly the CFL limit. The momentum increments from the mid-level convection scheme are only just stable at this limit. If they were any larger or if there is any vertical diffusion in the increments then mid-level convective momentum transport would be unstable (Kershaw *et al* (2000)). Additional vertical diffusion may effectively be added by the interpolation process of the winds onto the theta grid and the interpolation of the momentum increments back onto the U and V grids. This may be especially relevant over extreme orography.

5.2.2 Intermittency of deep convection

With a one-hour CAPE timescale deep convection is very intermittent. Fig 21 shows a timeseries of precipitation, updraught mass flux, and parcel buoyancy over one day at every timestep. The deep convective events occur at timesteps 1, 5, 8, 11, 14, 17, 20, 23, 27, 32, and 44. A number of mid-level convective events and a shallow convective event are also visible. The deep convective events at timesteps 1 to 32 initiate at ML 4 whilst the final event at timestep 44 initiates from ML 5. In the one-day shown here, deep convection never occurs on two consecutive timesteps. Indeed, over the 40-day period studied (1920 timesteps) there were only 11 occasions when full deep convection occurred on consecutive timesteps; this equates to less than 3% of deep convective events. The frequency of the time between consecutive deep convective events is shown as the red line in Fig 22. After a deep convective event there is typically between 2 and 5 timesteps before the next event.

Deep convection very rarely occurs on two consecutive timesteps because each deep convective event generates a convective inhibition that prevents deep convection from occurring on the next timestep. The process can be seen in the parcel buoyancy shown in Fig 21. Each time deep convection occurs, a single level convective inhibition is generated one level above the initiating level. It is generated by the deep convection cooling from the surface up to and including the initiation level (NTML) and warming above the initiation level. The convective inhibition is destroyed over time by the boundary-layer and the radiation schemes warming below the inhibition and the boundary-layer scheme cooling at the inhibition.

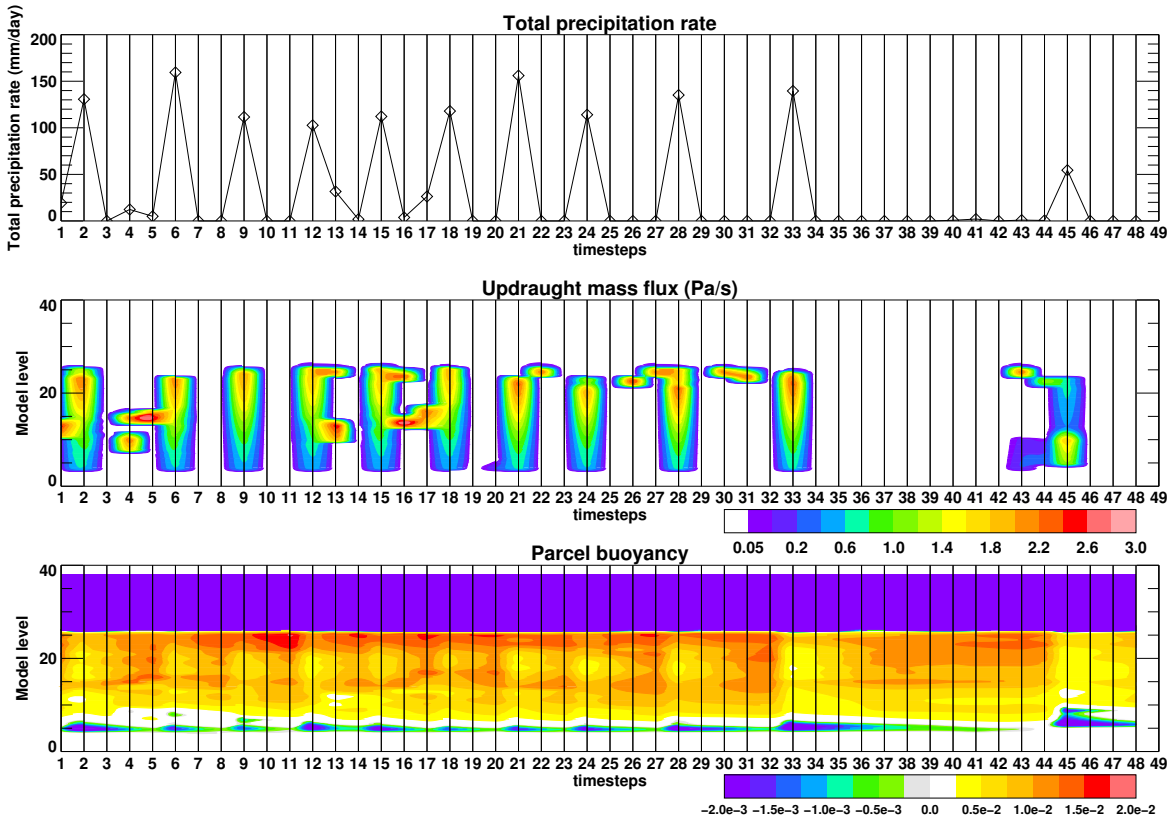

Figure 21: Timeseries of total precipitation rate (mm/day) (top); Updraught mass flux (Pa/s) (middle); and the buoyancy of a parcel lifted from model level one (bottom). The plots of buoyancy and updraught mass flux are slightly deceptive because of the contouring in the plotting software. The diagnostics don't vary smoothly over sub-timestep timescales instead they have discrete values at each timestep.

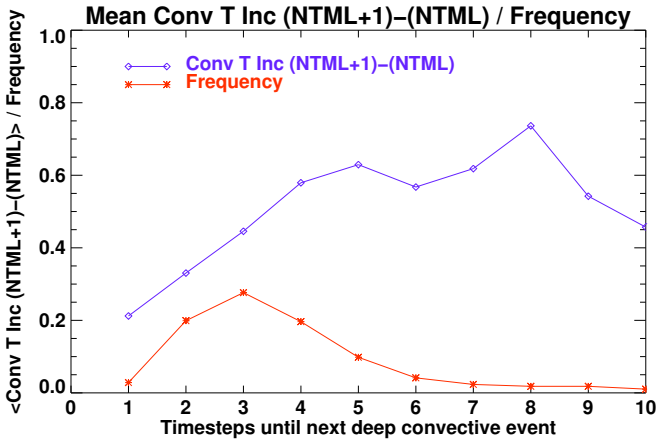

Figure 22: The mean convective inhibition as a function of the number of timesteps until the next deep convective event in K (blue); and the frequency of the number of timesteps between deep convective events (red). Deep convective events that have terminated early (see Section 5.2.3) have been excluded from this analysis.

An example of this process is shown in Fig 23. Deep convection initiates from ML 4. At this level and below, the convection scheme cools the environment through the formation of the updraught parcel, the detrainment of downdraught air, the evaporation of non-downdraught precipitation and the BL mixing of the convection increments. At ML 5 and above the convection scheme warms the environment through the compensating subsidence.The net result is that a convective inhibition is generated at ML 5. Over the next two timesteps the magnitude of the inhibition is reduced by a combination of warming at ML 1 by the longwave radiation and advection, and cooling at ML s5 by the advection and the boundary layer scheme. By the fourth timestep the convective inhibition has been reduced enough to allow deep convection to occur.

Fig 22 shows the mean magnitude of deep convective event generated inhibitions as a function of the number of timesteps until the next deep convective event. The inhibition is defined to be the difference in the convective temperature increment at one level above the initiation level (NTML+1) and at the initiation level (NTML). In general, there will be a longer wait until the the next deep convective event for a strong event than for a weak one. The magnitude of the convection inhibition is directly related to the strength of the deep convective event, i.e. a stronger deep convective event will generate a larger inhibition. After a strong event there will be time for the dynamics to generate CAPE and increase the relative humidity of the troposphere through vertical advection. However, the strength of deep convection is dependent on CAPE and the relative humidity and hence the next deep convective event will also be strong. There is therefore a feedback loop between the intermittency and the strength of convection.

5.2.3 Early termination of deep convection

As was stated in Section 5.1.1, deep convection often appears to terminate just a few MLs above where it initiates (Fig 24). The early terminating deep convection does tend to reduce the convective inhibition by warming the BL through the BL mixing of convective increments. It is therefore possible to have two or more consecutive early terminating deep convective events or early terminating deep convection followed by full deep convection.

The initial mass flux is at the low end of those observed for deep convection, i.e. 0.2Pa/s. However, over the 30-minute timestep this equates to 20% of the mass in the layer which does not appear to be particularly small. It should be noted that this is the mass flux after the CAPE scaling and that the mass flux used in the ascent, which uses the old buoyancy closure to determine the cloud base mass flux, will be different in magnitude but not in shape. The convecting plume sees the convective inhibition one ML above its initiating level. The convective inhibition is large enough to force the convecting plume to undergo forced detrainment at its initiating level. There is forced detrainment again at the ML of the convective inhibition. The calculated mass flux at the next ML is less than a minimum value (~0.03Pa/s) and therefore the convective plume terminates at the level of the convective inhibition. This explains the mechanics of how deep convection can terminate early but it doesn't explain why deep convection is initially diagnosed.

The diagnosis of deep convection is based on an undilute adiabatic moist parcel ascent. The diagnosis allows the ascent to continue even if the parcel is slightly negatively buoyant by an amount that is dependent upon the height of the surface mixed layer, the surface buoyancy flux and scaling velocity for momentum mixing in the surface mixed layer. Typically this value is between 0.2K and 1.0K (Lock, 2003). However, in the full ascent forced detrainment occurs when the buoyancy falls below a small positive critical value (see Section 3.2). This critical value is a function of layer thickness and typically is between 0.1K near the LCL and near the top of the troposphere and 0.16K in the mid-troposphere. In other words, the test for forced detrainment in the full ascent, which usually results in termination, is more stringent than the test for termination of convection in the diagnosis ascent. This inconsistency allows deep convection to be diagnosed but when the full ascent is done, which includes forced detrainment, the convective plume terminates after a couple of levels.

In the operational-forecast and climate models the convection scheme is substepped two and three times respectively. The convection scheme is substepped to relax the CFL criteria, and hence allow the convection scheme to do more work when under extreme conditions (i.e. gridpoint storms). However,

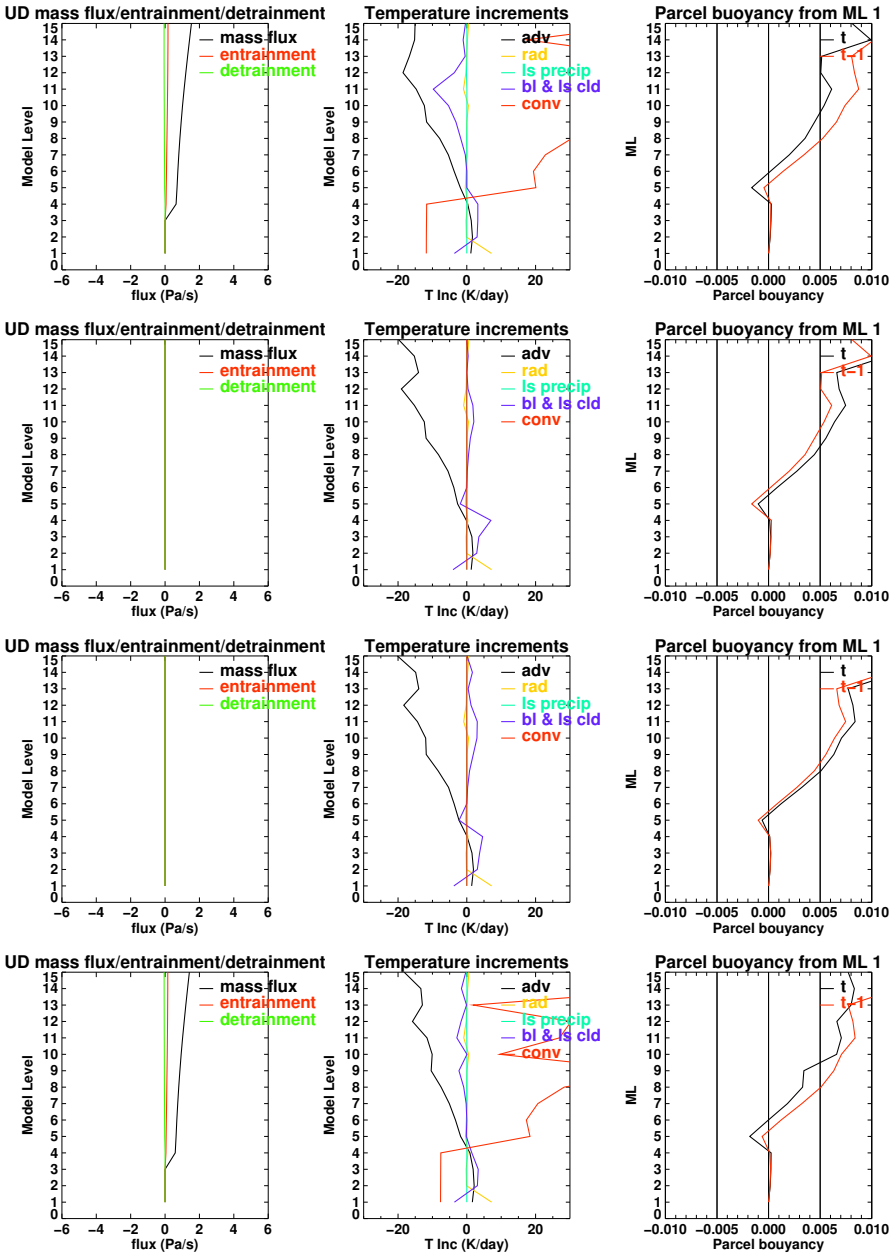

Figure 23: Sequence of 4 timesteps showing the formation and reduction of a convective inhibition. The updraught mass flux in Pa/s (left), the temperature increments in K/day (middle), and the parcel buoyancy in K/K (right) are shown for each of four timesteps (one per row).

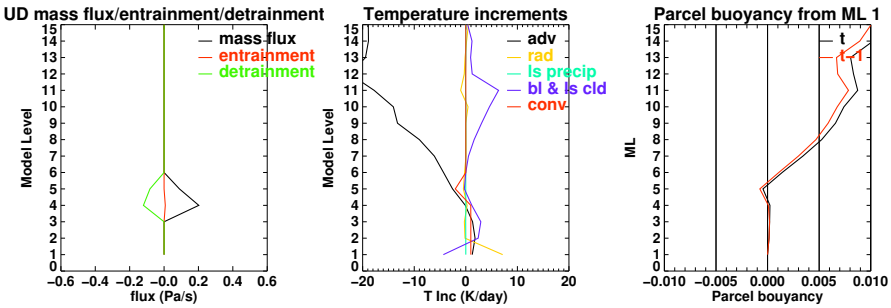

Figure 24: Example of the early termination of deep convection. The updraught mass flux in Pa/s (left), the temperature increments in K/day (middle), and the parcel buoyancy (right) are shown.

a convective inhibition is generated on the first substep and hence deep convection will often terminate on the second (or third) substeps after only a few MLs . When deep convection terminates early it cools the environment at the convective inhibition through the detrainment of moist air (Fig 24). Therefore, most of the benefit from substepping is probably due to early terminating deep convection eroding the convective inhibition on the second (and third) substeps, and hence reducing the intermittency of deep convection, rather than allowing the convection scheme to do more work in a single timestep by relaxing the CFL criteria.

5.2.4 Noise generated by forced detrainment

Convection normally acts to dry and warm the environment but at levels where there is forced detrainment, the convection tends to cool and moisten the environment. This is because the cooling and moistening due to detrainment of cloudy air and evaporation of cloud liquid water overcomes the warming and drying due to the updraught compensating subsidence. There is nothing incorrect with this as such, however, there is potentially a problem with the way in which forced detrainment is triggered, and the fact that it tends to operate in one layer. For example, Fig 25 shows deep convection with forced detrainment at ML 15. Throughout most of the profile the environment is warmed and dried. However, at ML 15 the environment is cooled and moistened by the forced detrainment to such an extent that the environment has become saturated. Whereas the original environment profiles of temperature and dew-point temperature were quite smooth, there is now a kink in both profiles. The generation of unrealistic single level features such as these is clearly undesirable.

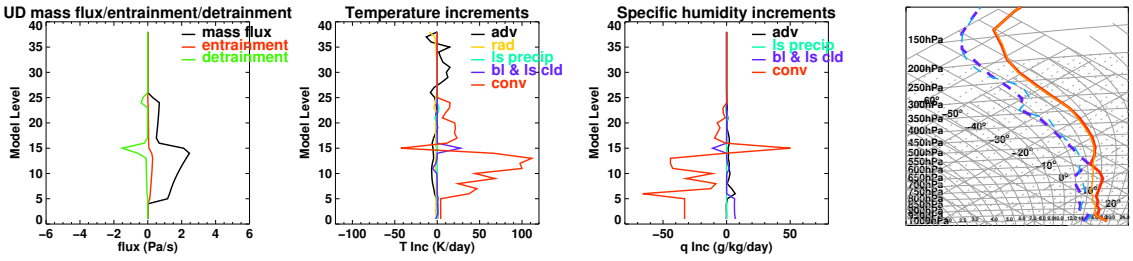

Figure 25: Example of the noise generated by forced detrainment. The updraught mass flux, entrainment and detrainment in Pa/s (left); the temperature increments in K/day (middle left); the specific humidity increments in g/kg/day (middle right); and tephigrams the start (orange and pale blue) and end (red and dark blue) of the timestep.

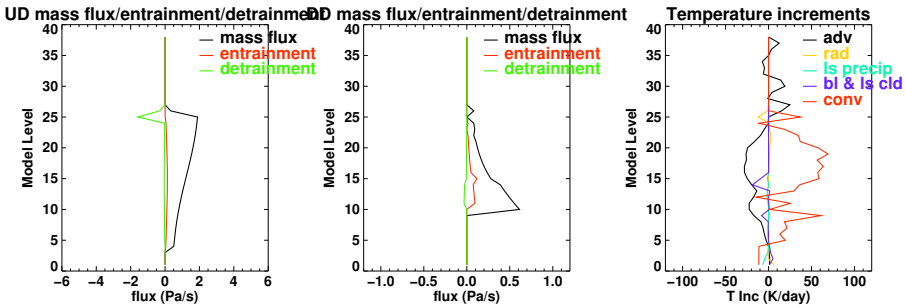

Figure 26: Example of early termination of deep convective downdraught. The updraught mass flux in Pa/s (left), the downdraught mass flux in Pa/s (middle), and the temperature increments in K/day (right) are shown.

5.2.5 Early termination of downdraughts

Downdraughts provide an important feedback from convection to the sub-cloud layer (Raymond (1995)). However, many downdraughts terminate before they reach the lowest levels (see Section 5.1.2). In particular, the downdraughts appear to preferentially terminate at about ML 9 (~800hPa), e.g. Fig 26.

The downdraught's negative buoyancy is maintained only by the evaporation of precipitation. The precipitation that is available for evaporation on a model level comes from the downdraught's unevaporated precipitation from the model level above and from the precipitation that has been transferred from the updraught into the downdraught at the current model level (See Section 3.3). The source of updraught precipitation which is available for transfer is only that which was created on the current model level. However, precipitation is only created in the updraught when the convective cloud liquid water exceeds 1.0g/kg (See Section 3.2). Therefore, precipitation will not start to be produced at cloud base but rather at a higher level. It is not possible to obtain the precipitation generated in the updraught as a diagnostic in the UM, therefore, the precipitation generation was estimated using an undilute parcel ascent from ML 1. This method indicates that an undilute parcel only begins to produce significant amounts of precipitation at around ML 8 (It should be noted that relative to an undilute parcel, a dilute parcel would produce less precipitation, and would only start to produce precipitation at a slightly higher level, because of the entrainment of relative dry environmental air). However, even if the amount of precipitation available to the downdraught is increased (by allowing the precipitation in the updraught to accumulate by falling from higher levels) the downdraughts still terminate early. This result and the large amount of surface precipitation produced suggests that there is still a significant amount of unevaporated precipitation in the downdraught when it terminates.

Except for allowing the downdraught to become slightly buoyant before termination, the current scheme ignores the water loading due to the unevaporated precipitation in the calculation of the downdraught's buoyancy. Preliminary tests indicate that including the water loading term greatly reduces the proportion of downdraughts that terminate before reaching lowest levels (this further supports the suggestion that currently downdraughts contain significant amounts of unevaporated precipitation when they terminate early). Therefore, it is suggested that the inclusion of the water loading term is essential to improve the behaviour of the downdraught scheme.

5.2.6 Boundary layer mixing

In the convection scheme the temperature, humidity and momentum increments are mixed between ML 1 and NTML. Hence the increments are always constant between ML 1 and NTML. It should be noted that NTML is the ML where shallow and deep convection are initiated from. The increments are mixed so that the convection scheme has a neutral effect on the stability of the BL; it is considered undesirable to have the convection scheme and the boundary-layer scheme in competition. However, the mixing of

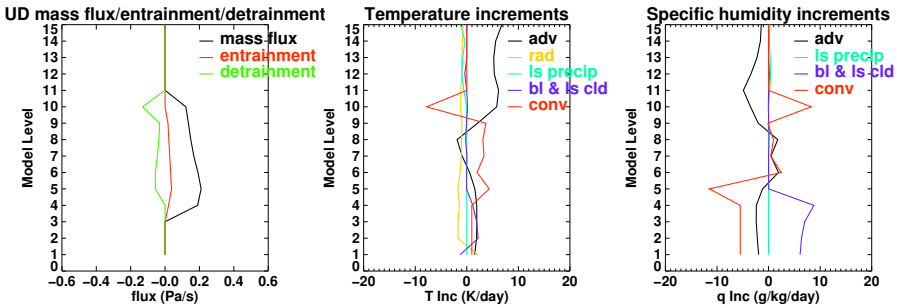

Figure 27: Example of the shallow convection boundary-layer mixing.The updraught mass flux in Pa/s (left), the temperature increments in K/day (middle), and the humidity increments in g/kg/day (right) are shown.

the convective increments in the boundary layer can produce some physically unrealistic increments. It is physically justified to mix the increments due to the formation of the convective parcel because the parcel is generated by the flux of heat and moisture out of the BL. However, the physical justification for mixing the increments from the other sources is unclear.

Downdraughts in the BL will cool and dry the environment and the evaporation of non-downdraught precipitation will cool and moisten the environment. Deep convection with downdraughts penetrating into the BL do always dry the BL as expected. However, in all the cases studied, deep and shallow convection dry the BL when there is no penetration of downdraughts into the BL (see the deep convection example in Fig 17 and the shallow convection example in Fig 15). The drying is due to the mixing of convective moisture increments. The drying due to the updraught compensating subsidence and the formation of the updraught parcel at NTML is larger than the moistening due to the evaporation of non-downdraught precipitation below NTML. Therefore when the increments are mixed the net effect is to dry between ML 1 and NTML.

There are also numerous cases of the shallow and deep convection warming the BL slightly for which there is no physical mechanism. These events occur when the warming from the updraught compensating subsidence at NTML is larger than the other factors that are acting to cool below at NTML and below. Therefore warming of the BL is often seen when there is no downdraught penetration and little or no precipitation for example during early terminating deep convection (Fig 24) or shallow convection (Fig 27). However, it is also seen during deep convective events when the updraught mass flux at NTML is large (e.g. Fig 25).

These examples illustrate cases where the sign of subcloud increments appears to be unphysical, however, it should be noted that in all cases the size and structure of the increments will be distorted by the mixing. The most significant term is probably the drying and warming from the updraught compensating subsidence at NTML which is mixed into the subcloud layer. It will result in a large systematic drying and warming of ML 1. Surface fluxes of heat and moisture are directly proportional to the temperature and humidity gradients between the surface and ML 1. Therefore, a spurious increase in drying of ML 1 will result in a spurious increase of the surface latent heat flux. In both shallow and deep convection, the BL mixing increases the amount of drying at ML 1 and hence increases the surface moisture fluxes. Aquaplanet experiments have shown that removing the convective BL mixing reduces the strength of convection in the tropics and reduces the amount of large-scale and convective precipitation.

5.2.7 Mid-level convection acting as deep convection

Mid-level convection can initiate near to the BL and not terminate until the mid- to upper-troposphere. In essence mid-level convection is performing deep convection. The only significant difference in the mass flux profiles is that mid-level convection is initiating several MLs above where deep convection would initiate. Fig 28 shows two examples of this. Deep convection typically starts between ML 3 and ML 5;

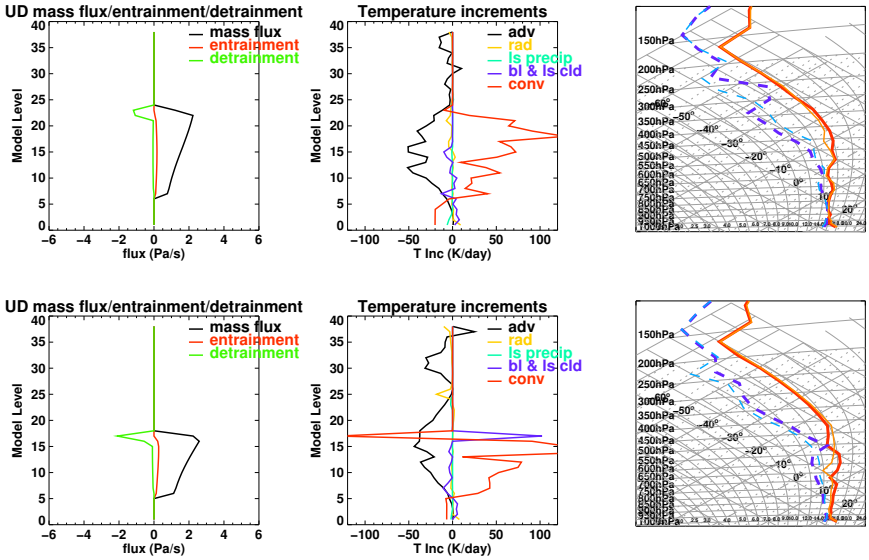

Figure 28: Examples of mid-level convection acting as deep convection. The updraught mass flux in Pa/s (left), the temperature increments in K/day (middle), and a tephigram (right) are shown.

in these cases mid-level convection has initiated at ML 7 and ML 6 and continued to ML 23 and ML 17 respectively. It should be noted that mid-level convection is not permitted to start at MLs where the BL scheme is operating, i.e. mid-level convection can only start above NTML.

In cases such as these, the atmospheric profile can obviously sustain convection throughout most of the free troposphere but deep convection is being inhibited by the processes discussed in Section 5.2.2. Therefore, the BL is being diagnosed as well-mixed and the mid-level convection is performing deep convection. Although there is nothing inherently wrong with this behaviour, it is questionable whether these cases should not in fact be diagnosed as deep convection. The effect on the environmental temperature and humidity profiles will be similar in both cases, however, the treatment of convective momentum transport is very different between deep and mid-level convection.

5.2.8 The role of deep convection in upper tropospheric humidity

Throughout most of the free troposphere the convective drying is balanced by advective moistening (Fig 6). However, the use of specific humidity tends to hide the details of the models behaviour in the upper troposphere because the values of specific humidity increments are very small. Fig 29 shows the time-mean relative humidity increments from the single equatorial point. (The relative humidity increments have been approximated by dividing the change in specific humidity by the saturated specific humidity). At the top of the troposphere the convection scheme is moistening the environment. Hence, rather than advection and convection being in balance as they are in most of the free troposphere, both are acting to moisten the atmosphere. The moisture supplied by the advection and convection is removed by large-scale precipitation. At the level where the convection scheme is moistening the environment there are persistent and significant amounts of large-scale cloud.

Fig 30 shows how these processes operate on a timestep by timestep level. It shows a timeseries of updraught mass flux, relative humidity, convective cloud, layer cloud and relative humidity increments from advection, large-scale precipitation, boundary-layer and large-scale cloud, and convection. Each time there is a deep convective event the relative humidity increases at the top of the upper troposphere (~ML 25) and decreases below this level. The convection scheme is producing this large amount of moistening by the forced detrainment of cloudy air at the terminating level. On the timesteps immediately following a deep convective event the large-scale precipitation drys the levels that the convection has just moistened. There are persistent and large amounts of large-scale cloud at the top of the troposphere. The

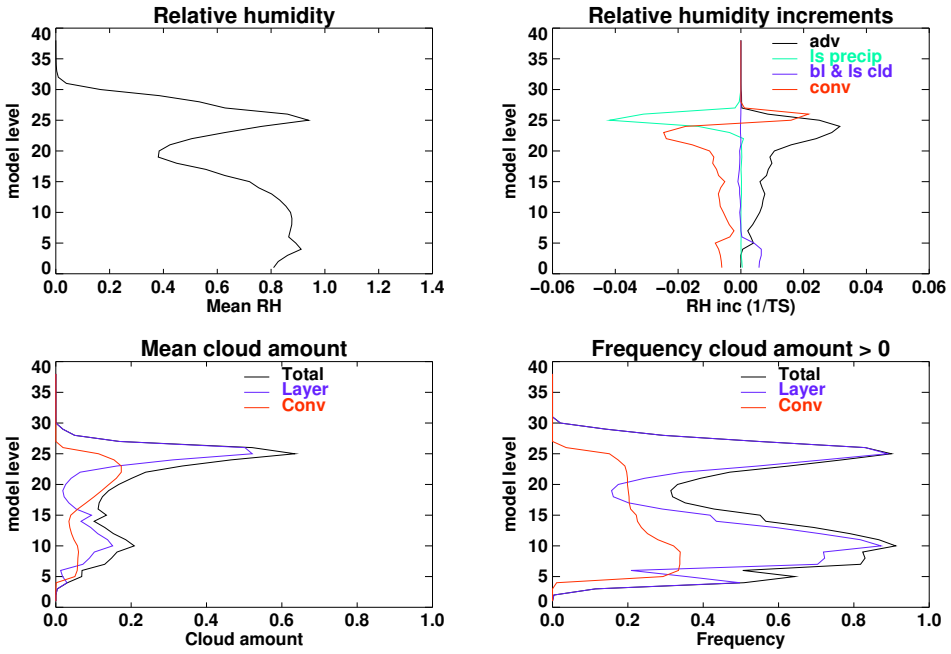

Figure 29: Time-mean profiles from the single equatorial point of relative humidity from (top left); relative humidity increments i.e. change in relative humidity per timestep (top right); fractional cloud amount (bottom left); and the frequency of non-zero cloud amount (bottom right).

amount of large-scale cloud reduces on the timestep on which there is deep convection because the total cloud amount is not allowed to be greater than 1.0. The moistening due to the advection is quite constant throughout the 12-hour period shown here.

In the region where convection is moistening the atmosphere the time-mean relative humidity is very high and it reaches a maximum of ~90% at ML 25. At ML 20 there is a minimum of ~40% in the time-mean relative humidity. The maximum and minimum in the relative humidity appear to coincide with the moist bias and dry bias in the full model (Fig 1). This suggests that the convective scheme is moistening too much near the top of the troposphere and not enough in the mid to upper troposphere. The drying in the mid to upper troposphere may be a symptom of too little detrainment of water vapour or condensate from the updraught coupled with a large updraught mass flux and its associated drying due to compensating subsidence. The only parametrized process that operates to moisten the environment is the mixing detrainment which is very small. Consequently when convection terminates and undergoes forced detrainment, it dumps all of its remaining parcel water vapour and condensate into the terminating layer and causes the excessive moistening seen here.

5.2.9 Balance between dynamics and physics

In the tropics between the LCL and the tropopause, there is a balance between the warming and drying due to the physics and the advective cooling and moistening if a large enough timescale or a large enough area is considered, e.g. see Fig 6. Almost all the warming and drying due to the physics comes from the convection scheme. Below the LCL, the main balance is between cooling and drying from the convection scheme, and warming and moistening from the boundary layer scheme but the advection, large-scale precipitation and radiation all have significant contributions. If short timescales and small areas are considered there will not in general be a balance in the temperature or the moisture fields. It should be noted that the imbalance between the dynamics and the physics could be a significant factor in RMS errors because it will result in significant amounts of temporal noise in the temperature and humidity fields.

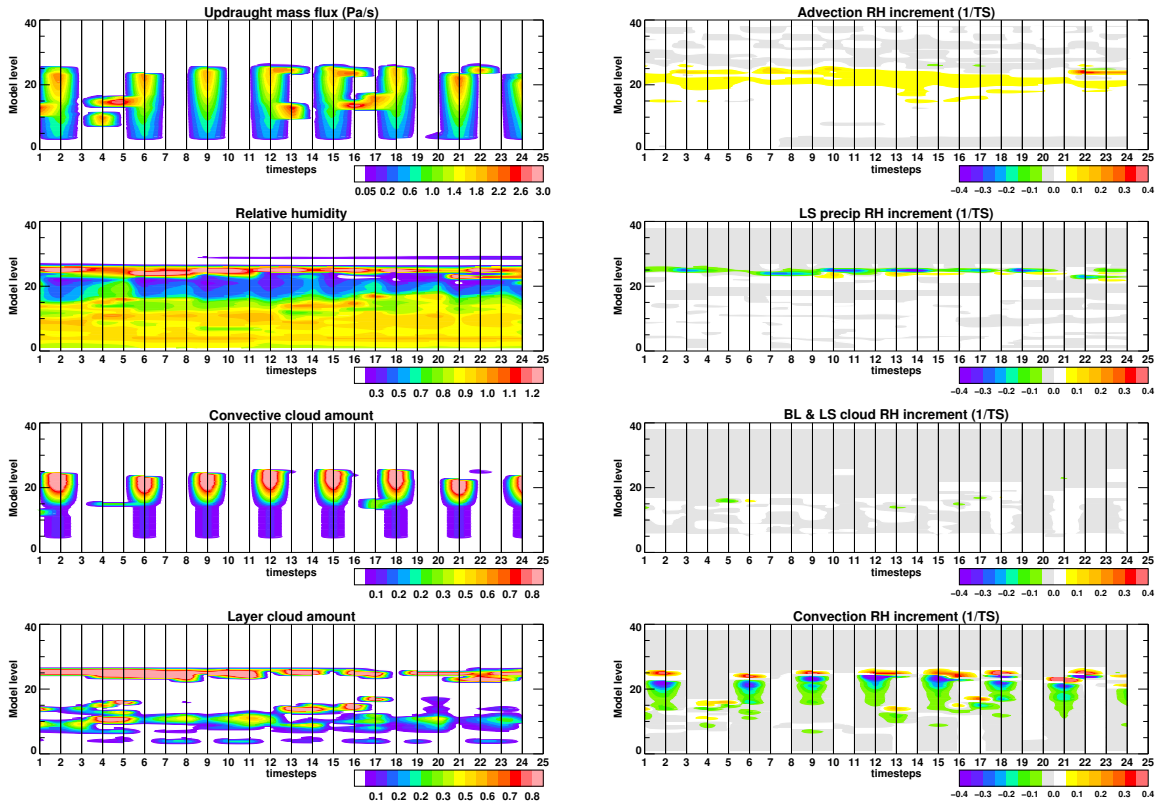

Figure 30: Timeseries of updraught massflux (top left); relative humidity (upper middle left); convective cloud amount (lower middle left); layer cloud amount (bottom left); relative humidity increments from advection (top right); relative humidity increments from large-scale precipitation (upper middle right); relative humidity increments from boundary-layer and large-scale cloud (lower middle right); and relative humidity increments from convection (bottom right).

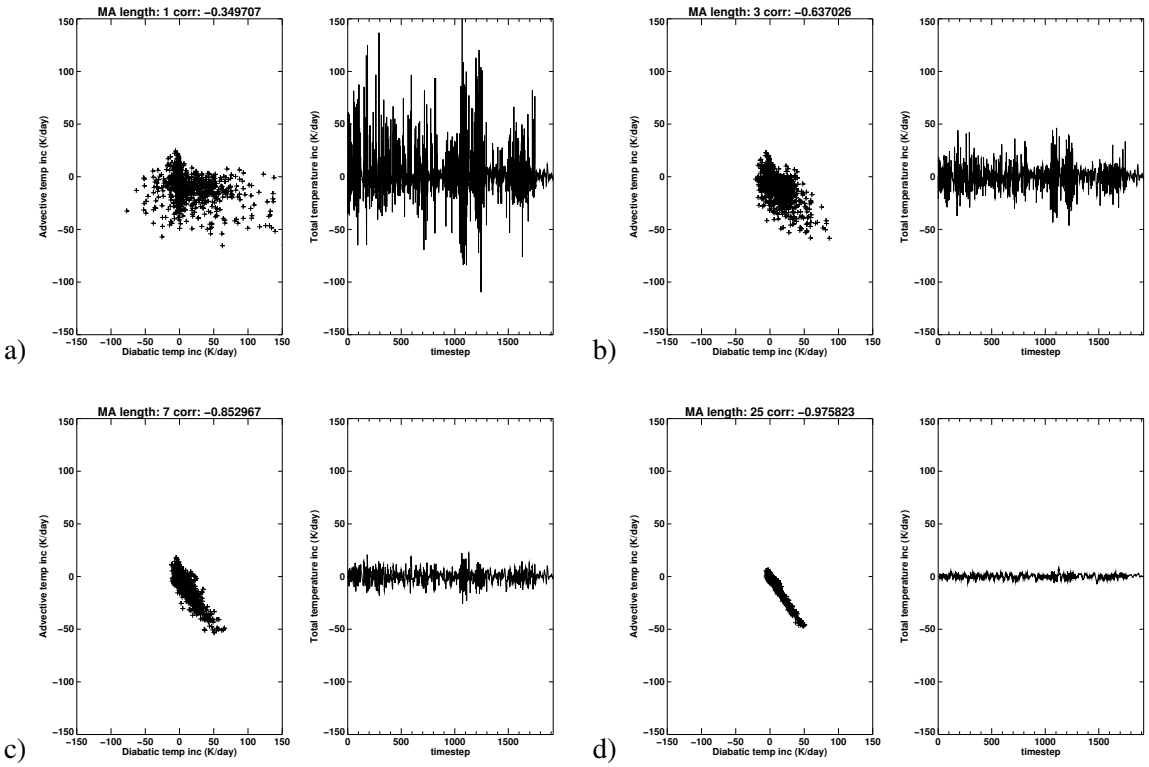

Figure 31: Advective temperature increments vs diabatic temperature increments (left) and the timeseries of total temperature increments (right) after: a) no filtering; b) a 3-point (1-hour) low-pass moving average filter; c) after a 7-point (3-hour) low-pass moving average filter; and d) a 25-point (12-hour) low-pass moving average filter.

Heat balance In general when a single gridpoint is considered timestep by timestep, the heating increments from the physics and dynamics are not in balance. In the case of the tropical free troposphere, the convective heating is not balanced by the dynamics over short timescales. Fig 31a shows a scatter plot of the advection temperature increment against the total physics temperature increment, and the timeseries of the total temperature increment, from ML 15 of the single point on the equator. The physics and the dynamics are clearly not in balance. There are imbalances between the dynamics and the physics of up to 150K/day, i.e. 3K in a single timestep. When it is considered that at this resolution, N48, this represents a gridbox of approximately 415km*550km*0.6km an increase of 3K in 30-minutes is not very physical. The standard deviation of the total temperature increment, which provides a convenient measure of the imbalance, at this level is 22.4K/day.

Fig 31b, c, and d are similar to Fig 31a except that low-pass moving-average filters of lengths 3, 7, and 25 timesteps have been applied to the total temperature increments. The low-pass moving-average filters greatly attenuate features on timescales less than 1 hour, 3 hours and 12 hours respectively. It can be seen that much of the imbalance is removed when a 3-timestep moving average is applied; in fact the standard deviation is halved to 10.7K/day. With the 7 and 25 timestep filters the standard deviation of the temperature increments are reduced to 5.7K/day and 1.9K/day respectively.

Fig 32 shows the standard deviations of the total, advection and physics temperature increments from ML 15 as a function of moving average length on both linear and logarithmic axes. The variances are related by $\sigma^2_{Total} = \sigma^2_{Advection} + \sigma^2_{Physics} + 2r\sigma_{Advection}\sigma_{Physics}$ where σ indicates a standard deviation and r is the correlation coefficient between the advection and physics increments (if the advection and physics were completely in balance then $\sigma_{Advection} = \sigma_{Physics}$, the increments would be completely anti-correlated, i.e. $r = -1$, and hence $\sigma_{Total} = 0$). Much of the variance in the total temperature increment occurs at short timescales of the order of a few timesteps and is due to a large variance in the

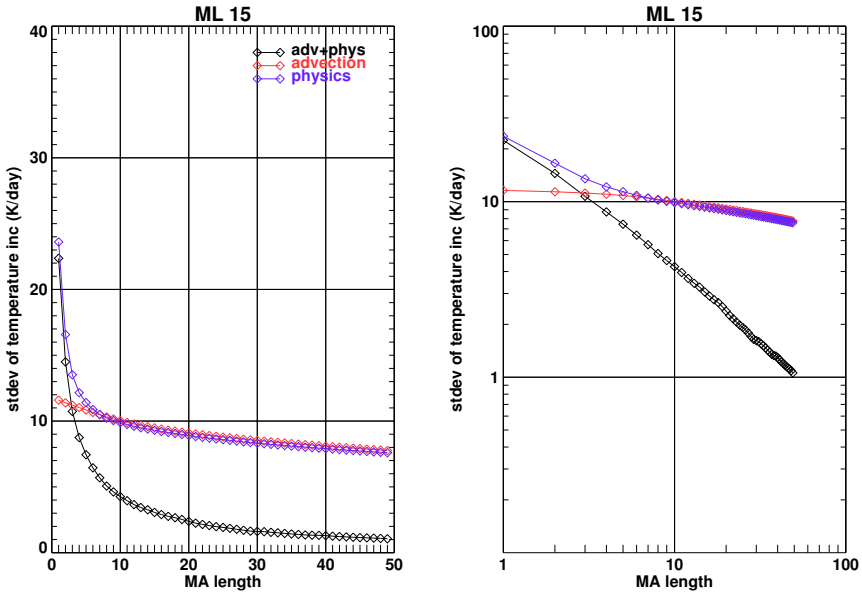

Figure 32: Standard deviation of total temperature increment, advection only and physics only as a function of moving average length. The left and right plots show the same data the only difference being the left plot is displayed on linear-linear axes and the right plot is displayed on log-log axes.

physics temperature increments at short timescales. That is, most of the imbalance at short timescales comes from the noise in the physics. For timescales greater than approximately 3 hours the physics and dynamics are approximately in balance and the variance in the total temperature increment is much less than that in the physics or the dynamics individually.

The imbalance between the physics and the advection is a common feature at all levels between the LCL and the tropopause. Fig 33 shows the standard deviation of total, advection and physics temperature increments as a function of ML with no filter, 3-timestep and 7-timestep moving average filters respectively. The imbalance between the physics and dynamics reaches a peak at ML 15, which is the freezing level.

Below ML 5, i.e. the LCL, the variance in the physics is the dominant factor in the variance in the total increment at the timescales less than 12 hours. For timescales of the order of a day or greater, the advection is a more significant factor. Above the tropopause, the temperature increments from the

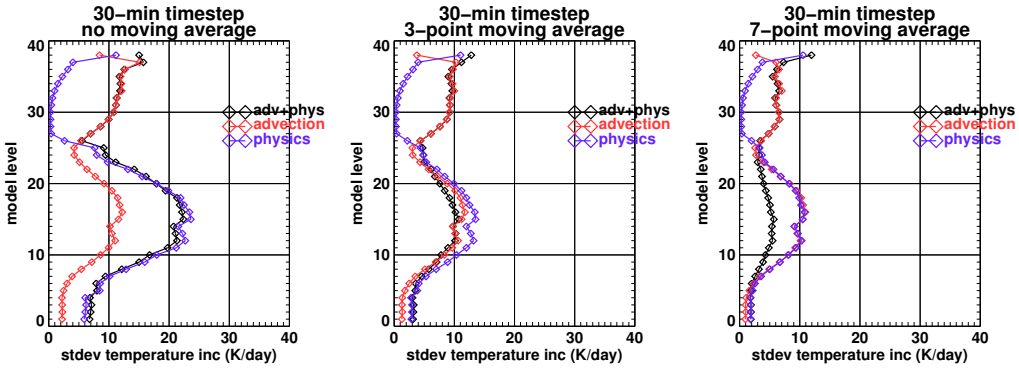

Figure 33: Standard deviation of total temperature increment, advection only and physics only as a function of model level after: no filtering (left); a 3-point (1-hour) low-pass moving average filter (middle); and after a 7-point (3-hour) low-pass moving average filter (right).

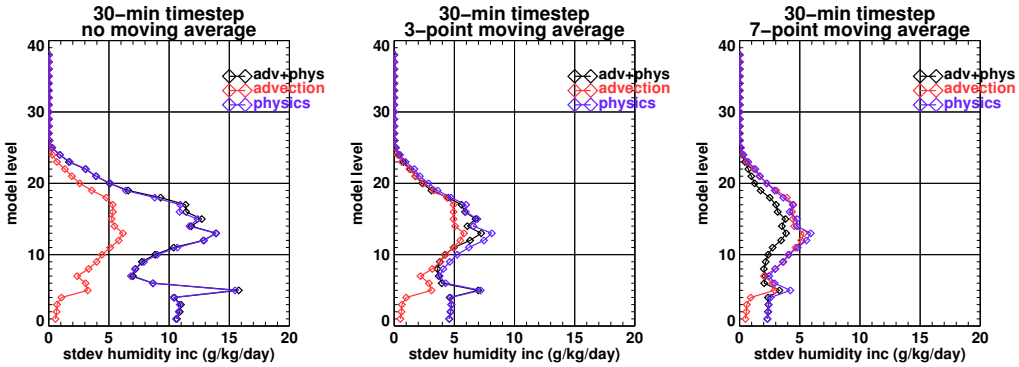

Figure 34: Standard deviation of total specific humidity increment, advection only and physics only as a function of model level after: no filtering (left); a 3-point (1-hour) low-pass moving average filter (middle); and after a 7-point (3-hour) low-pass moving average filter (right).

physics are dominated by the radiation. However, the variance of the physics increment is less than that of the advection increment. The variance of the advection increment reduces significantly with moving average length indicating that a lot of the variance in the advection exists on short timescales. Most of the variance in the advection increments is probably due to the convection induced gravity waves seen in Fig 18.

Moisture balance The humidity increments from the physics and advection are not in balance over short timescales (Fig 34). In the unfiltered case, the total variance is dominated by the variance in the physics at all MLs. Attenuating timescales less than one-hour halves the total and physics variance but has little effect on the advection variance. This indicates that much of the variance in the total and the physics increments exists over timescales of a few timesteps. It is necessary to remove timescales less than 6-hours (not shown) before there is (subjectively) a good balance between the physics and the advection in the free troposphere, i.e. the variance in the total increments are much smaller than those of the physics and advection increments. On subdiurnal timescales below the LCL, the total variance is dominated by the physics variance. At the ML 5, the LCL, there is a large peak in the variance of the unfiltered physics increments and a corresponding, but much smaller, peak in the advection increments. These peaks are still visible even after attenuating timescales less than 12 hours. The height of these peaks corresponds to the peaks in the mean convective drying and advective moistening (e.g. Fig 6) .

6 Sensitivity to timestep of the 4A convection scheme.

Additional runs using a 15-minute and 5-minute timestep were compared to the 30-minute timestep run. The aim of this work was to test the sensitivity of the 4A convection scheme and the model in general to timestep, to understand how some of the problems identified in the previous section respond to shortening of the timestep, and to examine the numerical convergence in the convection scheme.

6.1 Time-mean

6.1.1 Zonal averages

Shortening the timestep reduces the updraught mass flux in the deep tropics but increases the downdraught mass flux (Fig 35). There is also an indication that the updraught mass flux may be reaching a slightly higher level in the case of the 5-minute timestep. The convective precipitation rates are reduced in the deep tropics and elsewhere; the reduction is similar in both 5-minute and 15-minute cases. In the extratropics, the reduction in convective precipitation is balanced by an increase in the large-scale

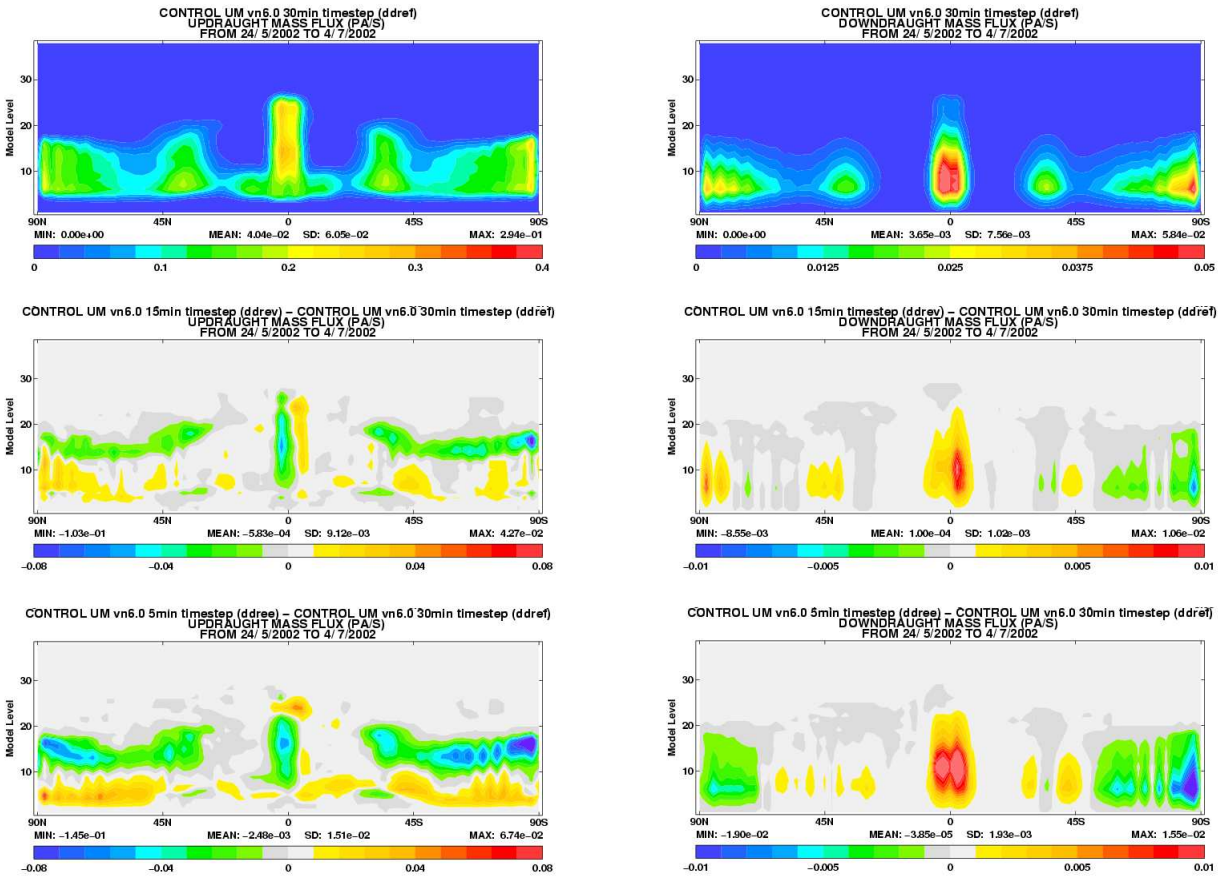

Figure 35: Left: The time- and zonal-mean convection updraught mass flux with a 30-minute timestep (top) in Pa/s; the difference between a 30-minute and 15-minute timestep (middle); and the difference between a 30-minute and 5-minute timestep (bottom). Right: The time- and zonal-mean downdraught mass flux with a 30-minute timestep (top) in Pa/s; the difference between a 30-minute and 15-minute timestep (middle); and the difference between a 30-minute and 5-minute timestep (bottom). Note that different scales are used for updraughts and downdraughts.

precipitation. In the deep tropics, there is only a small increase in large-scale precipitation that does not balance the decrease in convective precipitation, and hence, there is a net reduction of about 2mm/day in both cases (~10%). In the deep tropics, there is a reduction in convective heating (Fig 36) and convective drying (not shown). The reduction in convective heating and drying is similar for the 5-minute and 15-minute cases.

There is a small increase in convective cloud amounts in the tropics with the 15-minute timestep and a large increase with the 5-minute timestep. There are large changes in the distribution of large-scale cloud, and there is a large change in the balance between BL and large-scale cloud increments and the large-scale precipitation increments. These probably reflect a strong timestep sensitivity in the microphysics scheme; however, further discussion of this is outside the scope of this report.

Although the convective updraught mass flux, convective heating and drying are all reduced, the frequency at which both shallow and deep convection is diagnosed is increased, especially in the case of the 5-minute timestep (Fig 37). This suggests that the strength of each individual convective event is weaker on average with a shorter timestep. The increased frequency of deep convection is the probable cause of the increase in convective cloud amount.

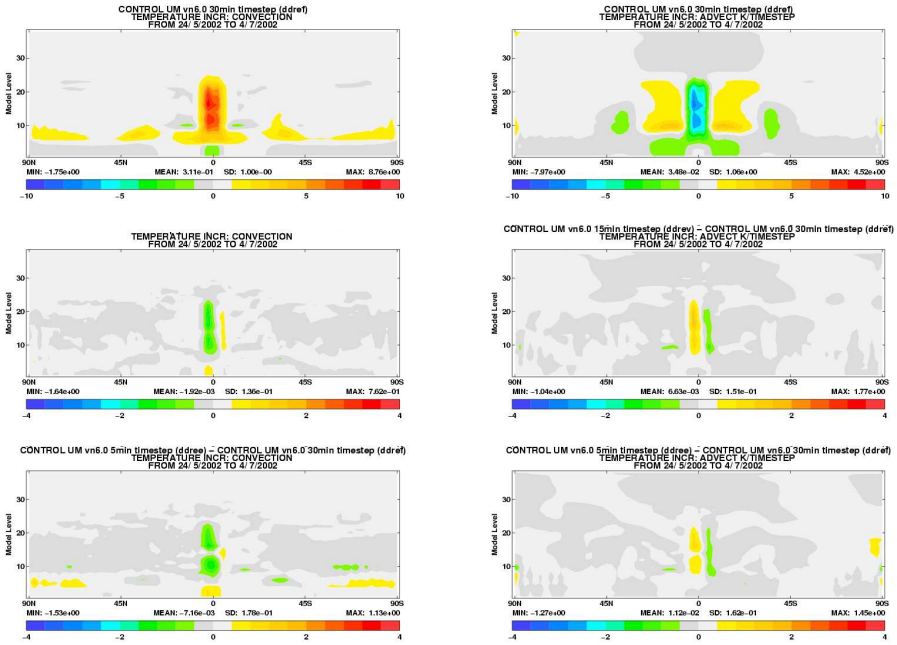

Figure 36: Left: The time- and zonal-mean convection increments with a 30-minute timestep (top) in K/day; the difference between a 30-minute and 15-minute timestep (middle); and the difference between a 30-minute and 5-minute timestep (bottom). Right: The time- and zonal-mean advection increments with a 30-minute timestep (top) in K/day; the difference between a 30-minute and 15-minute timestep (middle); and the difference between a 30-minute and 5-minute timestep (bottom).

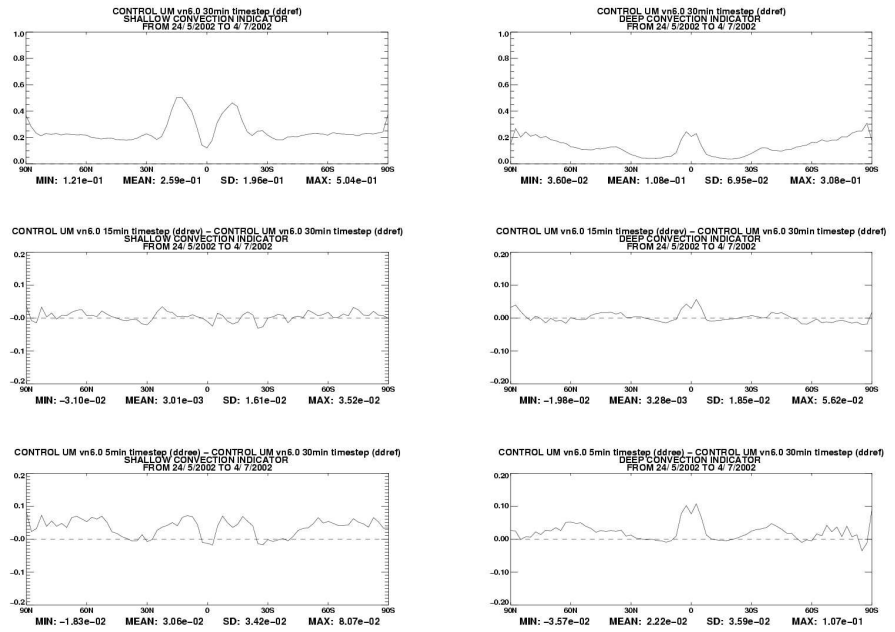

Figure 37: Left: The time- and zonal-mean distribution of shallow convection with a 30-minute timestep (top); the difference between a 30-minute and 15-minute timestep (middle); and the difference between a 30-minute and 5-minute timestep (bottom). Right: The time- and zonal-mean distribution of deep convection with a 30-minute timestep (top) in mm/day; the difference between a 30-minute and 15-minute timestep (middle); and the difference between a 30-minute and 5-minute timestep (bottom).

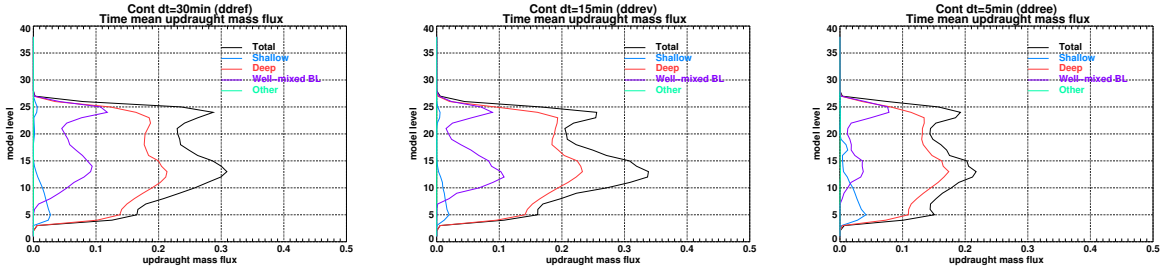

Figure 38: Vertical profile of time-mean updraught mass flux subdivided by convection type for 30-minute timestep (left), 15-minute timestep (middle), and a 5-minute timestep (right).

6.1.2 Single equatorial point

Again the data from every timestep at a single equatorial point was used to investigate the timestep sensitivity of the convection scheme and the model in more detail.

Updraughts As was seen in Fig 35, the time- and zonal-mean updraught mass flux tends to reduce when the timestep is shortened. Fig 38 suggests that this is dominated by a reduction in the contribution from the mid-level convection. There is much less mid-level convection being initiated throughout the troposphere when the timestep is reduced. A possible explanation for this is that the thermodynamic profile evolves much more smoothly with a shorter timestep and therefore, there is much less noise in the profile that can generate mid-level convection.

Convection type \ timestep	30-minute	15-minute	5-minute
Mid-level with BL III	89.2	63.0	30.0
Deep	38.0	4.7	0.2

Table 4: Proportion of deep and mid-level events whose mass fluxes exceed 90% of the CFL limit (Percent).

The proportion of mid-level events that reach the CFL limit reduces with timestep (Table 4) but even with a 5-minute timestep 30% of mid-level events reach the CFL limit at some level. At the top of the troposphere, there is a large increase in the mass flux per event when the timestep is reduced (not shown), and a large proportion of mass fluxes (up to 37%) still hit the CFL limit with a 5-minute timestep (Fig 39). This implies that the CFL limiter is a major factor in determining the mass flux of mid-level convection at the top of the troposphere. At the top of the troposphere, the increase in mid-level mass flux per event are more than compensated for by a large reduction in the frequency at which mid-level convection is initiated, and hence the time-mean mass flux is still reduced.

The deep convection updraught mass-flux per event is similar for all three timesteps (not shown). It perhaps indicates a slight reduction in the 5-minute case but there does not appear to be any large systematic changes with reduced timestep. The proportion of deep convective events that reach the CFL limit at one or more MLs falls dramatically with reduced timestep (Table 4). At the top of the troposphere ~25% of deep convective events reach the CFL limit with the 30-minute timestep. This falls to ~5% with a 15-minute timestep and almost zero with a 5-minute timestep. This implies that with a 30-minute timestep most events are only just exceeding the CFL limit. The frequency of early terminating deep convection does not seem to be affected by shortening the timestep.

There are not any systematic changes in the behaviour of shallow convection when the timestep is shortened.

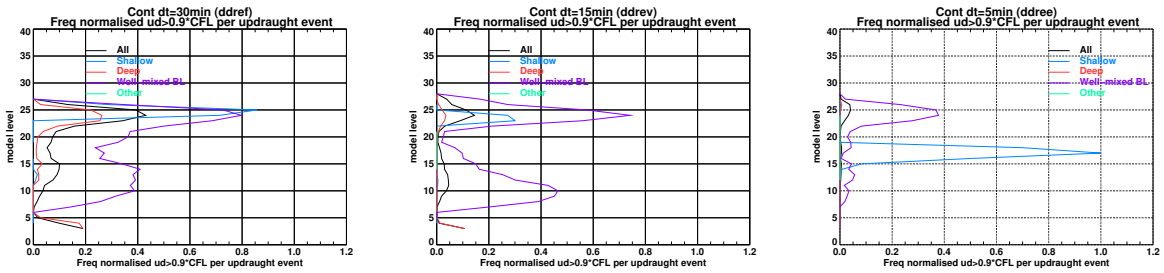

Figure 39: Frequency at which the updraught mass flux exceeds 90% of the CFL limit subdivided by convection type for 30-minute timestep (left), 15-minute timestep (middle), and a 5-minute timestep (right).

Downdraughts As with 30-minute timestep case, the downdraught mass flux in the 15-minute and 5-minute cases is dominated by deep convection. Although there is a small systematic increase of zonal- and time-mean downdraught mass flux on the equator (Fig 35) there is no such pattern visible in the time-mean from the single point. However, it should be noted that this is a single point and some variability should be expected. There are no significant differences in the time-mean mass flux per event for the deep convective downdraughts. Fewer downdraughts associated with mid-level convection are initiated probably reflecting the reduction in the frequency of mid-level convective events. Shortening the timestep reduces the frequency at which downdraughts initiate and terminate in the mid- to upper-troposphere. This is probably due to the smoother evolution of thermodynamic profile. The peak at ML 9 appears to be unaffected by timestep.

6.2 Timestep sensitivity of the temperature and moisture balance

Over timescales of a single timestep, the imbalance between the advective and physics heating rates are very similar with 30-minute and 15-minute (first row in Fig 40) but there is a small reduction in the imbalance when the timestep is shortened to 5-minutes. The variance in the physics increments dominates the total variance. Although the balance in heating rates are similar for all timesteps, it should be noted that the temperature imbalance over a timestep in absolute terms is obviously less with a shorter timestep. The temperature profile will therefore evolve more smoothly with a shorter timestep.

The imbalance between the physics and dynamics was compared over consistent timescales by time averaging the increments. For example, to compare the imbalance over a 30-minute timescale, the 30-minute timestep increments were not averaged, the 15-minute timestep increments were averaged with a 2-point moving average, and the 5-minute timestep increments were averaged with a 6-point moving average (second row of Fig 40). At these timescales there is a systematic reduction in the imbalance with reduced timestep. Throughout the free troposphere the imbalance relative to a 30-minute timestep is approximately halved with a 15-minute timestep and quartered with a 5-minute timestep; this suggests that it is a less than linear reduction in the imbalance with timestep. At timescales of 3-hours there is a reasonable balance between the physics and advection with 30-minute, 15-minute and 5-minute timesteps.

A similar situation is seen in the balance in the moisture increments. On 30-minute timescales throughout the free troposphere, the imbalance relative to a 30-minute timestep is approximately halved with a 15-minute timestep and quartered with a 5-minute timestep. However, even with 5-minute timestep the variance of the total increment is similar to that of the physics alone. Whereas with the temperature increments a subjectively good balance is achieved for all model timesteps on 3-hour timescales, with the humidity increments a good balance is only achieved at timescales greater than about 6-hours.

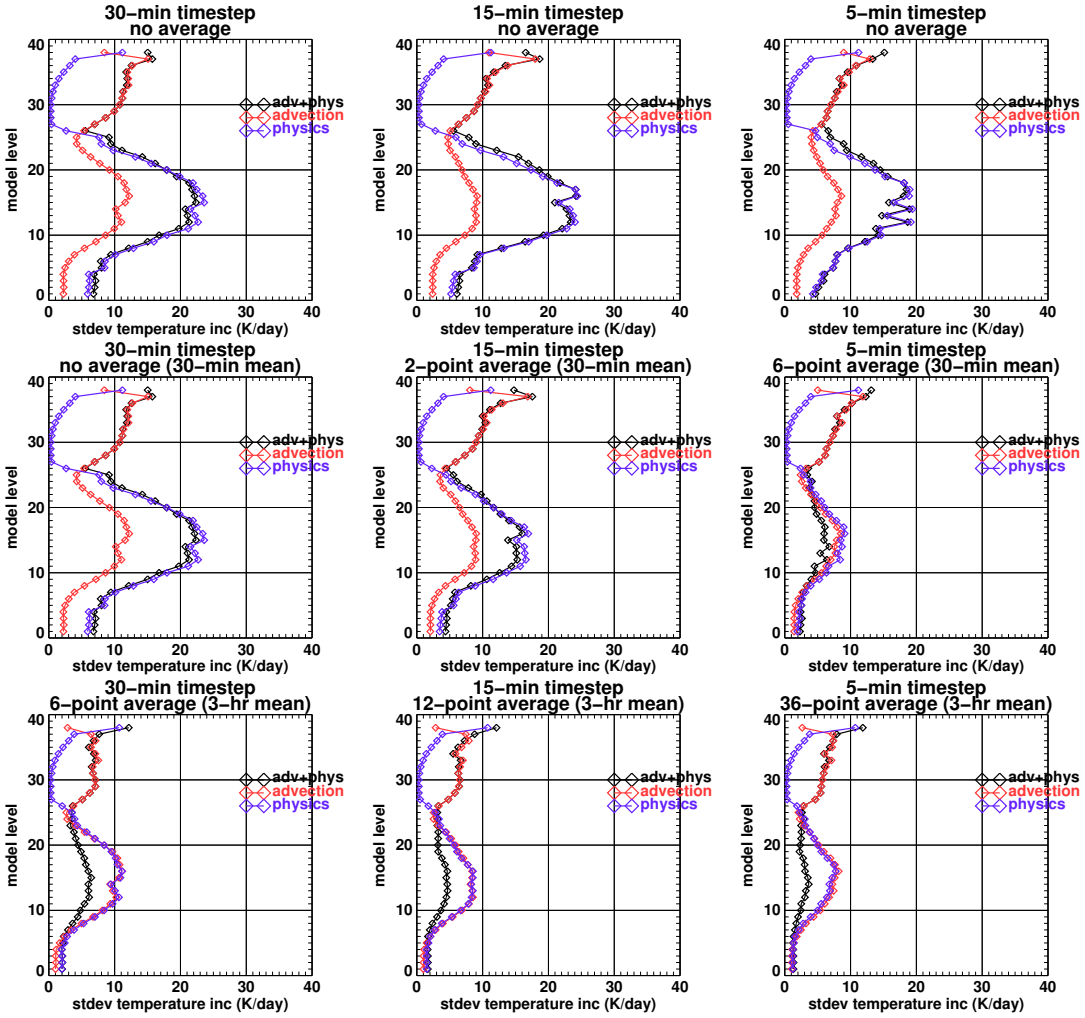

Figure 40: Standard deviation of total temperature increment, advection only and physics only as a function of model level and split by model timestep and averaging period: the left hand column has a 30-minute model timestep, the middle column has a 15-minute model timestep, and the right hand column has a 5-minute model timestep; the first row shows the standard deviations with no filtering, the second column the standard deviations after applying a 30-minute moving average, and the third row the standard deviations after applying a 3-hour moving average.

7 Conclusions

For some time the UM has had a persistent forecast error structure in the tropics. The structure of temperature biases, humidity biases, and the precipitation errors visible in forecasts suggest that the convection scheme may be a large component of the problem. The aquaplanet configuration was used to examine in detail the tropical behaviour of the UM focusing on the convection scheme. The aquaplanet proved to be a very useful methodology for this task because: there is a full interaction of physics and dynamics; it runs relatively quickly; it has a simple climate; and a single gridpoint is reasonably representative of a the aquaplanet's zonal mean because of the zonal symmetry. The aquaplanet model has allowed the identification and investigation of a number of issues that are listed below.

7.1 General behaviour of the convection scheme

7.1.1 Behaviour of mid-level convection

- Mid-level convection is a major contributor to the total updraught mass flux in the deep tropics (~30% of the total mass flux) but contributes little to the total downdraught mass flux.
- Mid-level convection tends to operate in two distinctive modes. Firstly, it can operate in a similar manner to deep convection, i.e. starting from the BL and convecting over a deep layer. Secondly, mid-level convection can start in the mid- or upper-troposphere and convect over a small number model levels (typically 2 to 4).
- When mid-level convection operates in mid- or upper-troposphere the mass fluxes are often very large and frequently reach the CFL limit even with a timestep as small as 5-minutes. This indicates that there is a serious flaw with the formulation of the CAPE closure when applied to this form of mid-level convection. The cause of the very large mass fluxes is a combination of the parcel's initial temperature perturbation and the dry adiabatic environment. This is exacerbated by high RH reducing the CAPE timescale.
- Large mid-level mass fluxes can also generate large momentum increments that can potentially create numerical instabilities in the model.
- Large mid-level mass fluxes can generate very large temperature and humidity increments that result in unrealistic environmental profiles of temperature and humidity.
- When mid-level convection operates in a similar manner to deep convection, i.e. starting in or near the BL and convecting over a significant depth, the mass fluxes are often large because of a combination of large environmental CAPE and a relatively short CAPE timescale that is further reduced by high environmental RH. The parcel's initial temperature perturbation is insignificant in these cases.
- In the time mean, mid-level convection contributes relatively little to the temperature and humidity increments in the mid- and upper-troposphere.
- Although there are obviously a number of problems associated with mid-level convection it is necessary for the model's stability. Switching off the mid-level convection quickly results in the model crashing due to the development of numerical instabilities.

7.1.2 Behaviour of deep convection

- Deep convection is the largest contributor to the updraught mass flux in the deep tropics and is responsible for almost all the total downdraught mass flux.

- Deep convection also produces very large mass fluxes. The mass fluxes frequently reaches the CFL limit with a 30-minute timestep but unlike mid-level convection rarely does when the timestep is shortened to 5-minutes. The cause of the large mass fluxes is a combination of intermittency of deep convection, which allows CAPE to build up in between convective events, and a relatively short CAPE timescale that can be further reduced by high environmental RH.
- The large mass fluxes can generate very large temperature and humidity increments but in general do shift the thermodynamic profile closer to a moist adiabat.
- Deep convection is very intermittent. The intermittency is due to deep convection generating a single level inhibition one model level above the initiation level. A stronger deep convective event will generate a larger inhibition which will take a longer time to be eroded. Consequently, stronger deep convective events have a longer mean time until the next event.
- Deep convective events often terminate after only a few model levels because of a mismatch between the parcel ascent in the diagnosis of cumulus convection and the full parcel ascent.
- Much of the benefit of substepping the convection scheme comes from early terminating deep convection eroding the convective inhibition on the second (or third) substeps and hence reducing the intermittency of deep convection.
- The structure of the moisture tendencies from deep convection is consistent with moisture biases observed in the deep tropics within the full model.
- The maximum in relative humidity at the top of the troposphere is caused by deep convection detraining large amounts of moisture where it terminates.
- The minimum in relative humidity in the mid- to upper troposphere is caused by deep convection's large updraught mass fluxes drying the environment through compensating subsidence and too little detrainment of moisture.

7.1.3 Generic behaviour

- Forced detrainment can create noise in the thermodynamic profile in the case of both mid-level and deep convection due to its tendency to be triggered over only a single level.
- Downdraughts frequently terminate before reaching the surface. There is an apparent tendency to terminate at around ML 9 (~800hPa) which is due to the lack of precipitation available for transfer into the downdraught and the absence of water loading in the downdraughts buoyancy calculation.
- The mixing of the convective increments in the BL can produce increments that have no physical justification. The mixing acts to produce spurious drying of the BL. A consequence of the drying is an increase in the surface moisture flux.
- Over a single 30-minute timestep the temperature and humidity increments from the physics and dynamics are not in balance. A good balance is only achieved over timescales greater than about 3-hours from the temperature increments and about 6-hours for the humidity increments.
- In the troposphere over timescales of a single timestep, most of the variance in the total temperature and humidity increments comes from the variance in the physics increments.

7.2 Timestep dependence

- Shortening the timestep reduces the updraught mass flux in the deep tropics but increases the downdraught mass flux.

- Most of the reduction in updraught mass flux comes from a reduction in mid-level convection. Deep convection is actually diagnosed more frequently but the mean strength of each event is reduced.
- Shortening the timestep leads to a smoother evolution of the thermodynamic profile.
- The reduction in mid-level convection is probably due to the smoother evolution of the thermodynamic profile .
- The total precipitation rate in the deep tropics is reduced by about 10% in both the 15-minute and 5-minute timestep cases relative to the 30-minute timestep case.
- The frequency at which deep convection reaches the CFL limit is greatly reduced when the timestep is reduced to 15-minutes and is almost zero when the timestep is shortened to 5-minutes. However, mid-level convection still frequently reaches the CFL in the upper troposphere even with a 5-minute timestep.
- The balance between large-scale precipitation and large-scale cloud increments appears to be very sensitive to the timestep.
- The early termination of deep convection and the early termination of downdraughts are unaffected by timestep.
- Timescales greater than about 3-hours for the temperature increments and 6-hours for the humidity increments are still required to achieve a good balance between the physics and dynamics.

8 Recommendations and future work

1. The current form of CAPE closure for mid-level convection needs to be reassessed. It may be appropriate to mid-level convection when it is acting as deep convection but is clearly not appropriate when it is operating over just a few levels in the mid- or upper-troposphere. Potential changes could include the following:

   (a) Altering the calculation of CAPE such that it no longer includes the contribution from the initial perturbation. This would make very little difference to the calculation of CAPE when there are significant amounts of real CAPE, i.e. deep convective or mid-level acting as deep convective cases.

   (b) Removing the CAPE timescale dependence on RH for mid-level convection starting in the mid- or upper-troposphere.

   (c) Using a different closure for mid-level convection depending on whether it is operating as deep convection or convecting over a few levels in the mid- or upper-troposphere. If mid-level convection starts in the mid- or upper-troposphere then a more appropriate closure could be used, e.g. a buoyancy closure or a closure based on the large-scale vertical velocity.

2. The current form of the mid-level convection CMT needs to be reassessed. Ideally, when mid-level convection is acting as deep convection then the CMT should be more consistent with that of deep convection.

3. The CFL limiter on the mass flux should be reduced slightly, e.g. from 100% of the layer mass to 95% of the layer mass in the convection timestep. This should mitigate the tendency of the mid-level convection CMT to become unstable whilst not significantly limiting the work that the convection scheme is able to do.

4. The dependence of the CAPE timescale on RH should be limited such that the CAPE timescale cannot be set to less than the convective timestep.

5. The mixing of the convective increments in the boundary layer should be reassessed.

6. The forced detrainment of updraught air over just a single model level, which is usually the terminating level, is far too abrupt. Other options that result in a more continuous detrainment profile should be considered. These could include the following:

   (a) Reformulating the balance between entrainment and mixing detrainment such that the mass flux reduces at higher levels and the forced detrainment becomes less significant.

   (b) Replacing the current fixed buoyancy excess at which forced detrainment operates with a more adaptive triggering function. Work on adaptive detrainment is currently being undertaken.

7. The termination conditions for deep convection should be reassessed. Potential changes could include the following:

   (a) A more accurate calculation of the undilute parcel properties.

   (b) Not permitting the termination of deep convection immediately after initiation.

8. The downdraught scheme should be reformulated to prevent the spurious early termination of downdraughts. This could be done by:

   (a) Allowing the precipitation to fall within the updraught and hence allowing the downdraught access to the accumulated precipitation.

   (b) Including water loading in the buoyancy calculation which will help to maintain the negative buoyancy of the downdraught.

9. The behaviour of the model, and the convection scheme in particular, should be compared to observations, cloud resolving models, single column models and other NWP models. This is currently being done as part of a GCSS working group 4 project.

The method of using very detailed, timestep by timestep diagnostics has proved to be very useful in identifying and investigating the behaviour of the convection scheme in a deep-tropical, oceanic situation. The method should be applied to other regimes where convection plays an important role, e.g. deep convection over land, shallow cumulus regions. Diagnostics that subdivide the convective increments into the individual processes (e.g. compensating subsidence, detrainment of cloudy air) should be developed. This would allow a more complete picture of the operation of the convection scheme.

References

Grant, A. L. M., and A. R. Brown, 1999: A similarity hypothesis for cumulus transports. *Q. J. R. Meteorol. Soc.*, **125**, 1913–1935.

Gregory, D., and P. R. Rowntree, 1990: A mass flux convection scheme with representation of cloud ensemble characteristics and stability dependent closure. *Mon. Wea. Rev.*, **118**, 1483–1506.

——, 1995: A consistent treatment of the evaporation of rain and snow for use in large-scale models. *Mon. Wea. Rev.*, **123**, 2717–2732.

Kershaw, R., A. L. M. Grant, S. H. Derbyshire, and S. Cusack, 2000: The numerical stability of a parametrization of convective momentum transport. *Q. J. R. Meteorol. Soc.*, **126**(569A), 2981–2984.

Lock, A., 2003: Bounday layer processes, option 6/8a: The parametrization of turbulent fluxes above the surface. Unified Model Documentation Paper 24, Met Office, FitzRoy Road, Exeter, EX1 3PB, UK.

Maidens, A., 2005: Convection scheme. Unified Model Documentation Paper 27, Met Office, FitzRoy Road, Exeter, EX1 3PB, UK.

Milton, S. F., I. Culverwell, G. Greed, and M. Willett, 2003: Improving tropical performance. i- diagnosing errors in the new unified model (cycle g27). Forecasting Research Technical Report 401, Met Office, FitzRoy Road, Exeter, EX1 3PB, UK.

Neale, R. B., and B. J. Hoskins, 2000: A standard test for agcms including their physical parametrizations: I: The proposal. *Atmospheric Science Letters*, **1**, doi:10.1006/asle.2000.0019.

Raymond, D. J., 1995: Regulation of moist convection over the west pacific warm pool. *J. Atmos. Sci.*, **52**, 3945–3959.

Appendix

Definitions of detailed timestep diagnostics.

- Column 1.
  - Row 1. Updraught mass flux (black, Pa/s), updraught entrainment (red, Pa/s) and detrainment (green, Pa/s).
  - Row 2. Downdraught mass flux (black, Pa/s), updraught entrainment (red, Pa/s) and detrainment (green, Pa/s).
  - Row 3. Updraught mass flux (black, fraction of layer mass/timestep) and downdraught mass flux (red, fraction of layer mass/timestep) normalised to the fraction of the mass in the layer, i.e. a value of one will mean all the mass is flowing from the layer in a single timestep.
- Column 2.
  - Row 1. The temperature increments (K/day) from the advection (black), radiation (yellow), large-scale precip (green), boundary-layer and large-scale cloud (blue) and convection (red).
  - Row 2. The humidity increments (g/kg/day) from advection (black), large-scale precip (green), boundary-layer and large-scale cloud (blue) and convection (red).
  - Row 3. Tephigram with the temperature at the end of this timestep (solid red), the previous timestep (solid orange), dew point temperature at the end of this timestep (dashed dark blue) and the previous timestep (dashed light blue).
- Column 3.
  - Row 1. The moist static energy (J/kg) at the end of this timestep (black) and the previous timestep (red).
  - Row 2. The moist static energy increment (J/kg/day) from advection (black), radiation (yellow), large-scale precip (green), boundary-layer and large-scale cloud (blue) and convection (red).
  - Row 3. The convective (red) and layer cloud fractions (blue) and the relative humidity (black).
- Column 4.
  - Row 1. The parcel buoyancy (i.e. fraction difference in virtual temperature) from a parcel lifted from ML 1 at the end of this timestep (black) and the previous timestep (red).
  - Row 2. A timeseries of the CAPE (red line) and the convective inhibition scaled by a factor of 100 (blue line) from a parcel lifted from ML 1. Plus and minus twelve timesteps, i.e. six hours with a 30 minute timestep, relative to the current time are shown. The convective inhibition is calculated to be the integral of the buoyancy between ML 1 and the level of free convection. And the CAPE is the integral of the buoyancy from the level of free convection to the level of neutral buoyancy. The LFC is determined by looking for the first time the parcel from ML 1 becomes positively buoyant after being negatively buoyant. If this never occurs then the LFC is set to ML 1. The LNB is found by looking for the *first* time the buoyancy becomes negative above the LFC. Because of this, if there is an inversion just above the LFC then the CAPE will be very small.
  - Row 3. A timeseries of the total precipitation rate (black, mm/day), 10*the surface sensible heat flux (blue, W/m2), and the surface latent heat flux (red, W/m2).

Model level	Height (m)	Mean pressure (hPa)	Mean temperature (K)	Mean potential temperature (K)
1	20.0	1008.7	298.7	298.0
2	80.0	1001.8	298.1	297.9
3	180.0	990.5	297.1	297.9
4	320.0	974.8	295.8	298.0
5	500.0	954.9	294.7	298.6
6	720.0	931.0	293.5	299.5
7	980.0	903.4	292.0	300.6
8	1280.0	872.4	290.4	302.0
9	1620.0	838.3	288.7	303.7
10	2000.0	801.6	286.9	305.6
11	2420.0	762.6	285.0	307.9
12	2880.0	721.8	282.8	310.4
13	3380.0	679.5	280.4	313.1
14	3920.0	636.2	277.7	316.0
15	4500.0	592.2	274.5	318.8
16	5120.0	548.1	271.5	322.4
17	5780.0	504.2	267.8	325.6
18	6480.0	460.9	263.7	329.0
19	7220.0	418.4	258.8	331.9
20	8000.0	377.0	252.9	334.2
21	8820.0	337.0	246.4	336.2
22	9680.0	298.6	239.3	337.9
23	10580.0	262.1	231.5	339.4
24	11520.0	227.5	223.2	340.6
25	12500.0	195.2	214.4	341.8
26	13520.0	165.4	206.1	344.6
27	14581.0	138.4	199.7	351.3
28	15694.5	114.2	197.3	366.6
29	16875.5	93.1	197.6	389.3
30	18138.5	74.9	199.7	418.6
31	19503.0	59.5	204.1	457.1
32	20990.0	46.5	210.0	504.3
33	22626.0	35.8	215.8	558.7
34	24458.5	26.8	220.7	620.4
35	26583.5	19.4	225.8	696.6
36	29219.0	13.0	230.3	795.5
37	32908.5	7.6	234.6	946.5
38	39255.0	3.1	264.8	1377.4

Table 5: Model theta level heights, average pressures, average temperatures and average potential temperatures. The average pressures and temperatures are 40-day time-means from the single equatorial point.

Process	Effect on environmental potential temperature		Effect on environmental humidity		Location
Updraught compensating subsidence	$\frac{M_k}{\Delta p_k}\left(\theta_{k+1}^{Env}-\theta_k^{Env}\right)$	warm	$\frac{M_k}{\Delta p_k}\left(q_{k+1}^{Env}-q_k^{Env}\right)$	dry	NTML (shallow or deep) or starting level (mid-level) to terminating level
Updraught mixing detrainment	$M_k\mu_k\left(\theta_k^{Par}-\theta_k^{Env}\right)$	warm or cool	$M_k\mu_k\left(q_k^{Par}-q_k^{Env}\right)$	moisten	NTML (shallow or deep) or starting level (mid-level) to terminating level
Updraught forced detrainment	$M_k\delta_k\left(\theta_k^{FDet}-\theta_k^{Env}\right)$	warm or cool	$M_k\delta_k\left(q_k^{FDet}-q_k^{Env}\right)$	moisten	Terminating level and where parcel buoyancy falls below threshold
Evaporation of detrained cloud liquid water	$-M_k\frac{L'}{c_p}\left(\mu_k+\delta_k\right)l_k^{Par}$	cool	$M_k\left(\mu_k+\delta_k\right)l_k^{Par}$	moisten	NTML (shallow or deep) or starting level (mid-level) to terminating level
Formation of updraught	$-\frac{M_{ntml}}{\Delta p_{ntml}}\left(\theta_{ntml}^{Par}-\theta_{ntml}^{Env}\right)$	cool	$-\frac{M_{ntml}}{\Delta p_{ntml}}\left(q_{ntml}^{Par}-q_{ntml}^{Env}\right)$	dry	NTML (shallow or deep) or starting level (mid-level)
Downdraught compensating upward flow	$\frac{M_k^{DD}}{\Delta p_k}\left(\theta_{k-1}^{Env}-\theta_k^{Env}\right)$	cool	$\frac{M_k^{DD}}{\Delta p_k}\left(q_{k-1}^{Env}-q_k^{Env}\right)$	moisten	Downdraught levels
Downdraught detrainment	$M_k^{DD}\eta_k\left(\theta_k^{DD}-\theta_k^{Env}\right)$	cool	$M_k^{DD}\eta_k\left(q_k^{DD}-q_k^{Env}\right)$	moisten or dry	Downdraught levels
Formation of downdraught	$-\frac{M_{init}^{DD}}{\Delta p_k}\left(\theta_{k-1}^{DD}-\theta_{k-1}^{Env}\right)$	warm	$-\frac{M_{init}^{DD}}{\Delta p_k}\left(q_{k-1}^{DD}-q_{k-1}^{Env}\right)$	dry	Downdraught initiation level
Change of phase of non-DD precipitation	$\pm gL_fP_k/\left(c_p\Pi_k\Delta p_k\right)$	cool	$-$	-	Freezing level. + if snow crosses freezing level and melts or - if rain crosses freezing level and freezes.
Evaporation/sublimation of non-DD precipitation	$-C_{conv}\frac{\left(L_cE_k^{local}+\left(L_c+L_f\right)S_k^{local}\right)}{\left(c_p\Pi_k\Delta p_k\right)}$	cool	$C_{conv}\left(E_k^{local}+S_k^{local}\right)/\Delta p_k$	moisten	Below cloud base

Table 6: Convective processes and their impact on the environment